

Dalton Transactions

Accepted Manuscript



This is an *Accepted Manuscript*, which has been through the Royal Society of Chemistry peer review process and has been accepted for publication.

Accepted Manuscripts are published online shortly after acceptance, before technical editing, formatting and proof reading. Using this free service, authors can make their results available to the community, in citable form, before we publish the edited article. We will replace this *Accepted Manuscript* with the edited and formatted *Advance Article* as soon as it is available.

You can find more information about *Accepted Manuscripts* in the [Information for Authors](#).

Please note that technical editing may introduce minor changes to the text and/or graphics, which may alter content. The journal's standard [Terms & Conditions](#) and the [Ethical guidelines](#) still apply. In no event shall the Royal Society of Chemistry be held responsible for any errors or omissions in this *Accepted Manuscript* or any consequences arising from the use of any information it contains.

Gadolinium-Containing Endohedral Fullerenes: Structures and Function as Magnetic Resonance Imaging (MRI) Agents

Kamran B. Ghiassi, Marilyn M. Olmstead, and Alan L. Balch*

Department of Chemistry, University of California, One Shields Avenue, Davis, CA, U. S. A.

E-mail: albalch@ucdavis.edu; Fax +1 (530) 752 2820; Tel +1 (530) 752 0941

Abstract

Gadolinium-containing endohedral fullerenes represent a new class of effective relaxation agents for magnetic resonance imaging (MRI). The range of different structures possible for this class of molecules and their properties as MRI agents are reviewed here.

Introduction.

Ton quantities of gadolinium have been administered to humans as medicinal diagnostic agents for use in magnetic resonance imaging (MRI).^{1,2} The presence of seven unpaired electrons in the Gd(III) ion make this ion the premier choice as a water relaxation agent in MRI applications. However, free, aquated gadolinium ions are toxic.³ These ions can inhibit calcium channels and have neurological and cardiovascular toxicity. In order to be used clinically, the gadolinium ion must be placed in a chelated environment that binds the metal tightly but allows water to interact with the unpaired spins of the gadolinium. The usual solution involves using polyfunctional ligands that strongly coordinate the Gd³⁺ ion, while allowing at least one water molecule to bind directly to the Gd³⁺. Figure 1 shows the structure of a complex of the type used in the many different commercial relaxation agents.⁴ The key elements in this drawing are the attachment of the polydentate ligand to the metal through amine and carboxylate functions and the presence of a single, coordinated water molecule.

Figure 2 illustrates a simple scheme that shows how water relaxation occurs in the vicinity of the gadolinium complex. The exchange of the coordinated water with bulk water is considered as the primary and best understood process that leads to effective relaxation of the water protons. In considering the design of gadolinium relaxation reagents one reads statements like: “In addition, at least one water molecule must be bound to the gadolinium centre (i.e. within the coordination sphere) and this will undergo rapid exchange with the water molecules of the surrounding solution to affect the relaxation time of all the solvent protons.”² However, exchange and relaxation may take place through interaction of water molecules in the second and subsequent hydration layers with the complex through hydrogen bonding and other means, but without direct coordination.

The escape of gadolinium from these chelates can result in an acquired disorder, nephrogenic systemic fibrosis (*NSF*, (not to be confused with NSF, the National Science Foundation)).^{5,6} This condition occurs in people with impaired renal function. Thus, the use of gadolinium relaxation agents is discouraged in individuals with kidney disease.

Endohedral metallofullerenes, closed carbon cages with metal atoms trapped within their confined space, offer an alternative means of binding a paramagnetic metal such as gadolinium.^{7,8,9} The closed network of carbon atoms prevents any leakage of the metal from the cage, while the molecule retains all of the physical properties of the metal confined inside. However, direct contact of a water molecule with a gadolinium atom on the inside cannot happen. If these endohedral fullerenes are to function as MRI contrast agents and they do (*vide infra*), the relaxation must occur through an outersphere mechanism. Numerous endohedral fullerenes have been prepared, purified and isolated, since the first report of their existence appeared.¹⁰ Here, we examine the gadolinium-containing endohedral fullerenes that have been discovered with particular attention to the structures of these intriguing molecules.

Gadolinium-Containing Endohedral Fullerenes.

Synthesis. Endohedral fullerenes are generated by the electric arc method in which graphite rods doped with a metal source, generally a metal oxide (Gd_2O_3 in the case of gadolinium-containing endohedrals), are vaporized in a low-pressure helium atmosphere.¹¹ In this arc, fullerenes are formed from smaller carbon fragments particularly C_2 units within a temperature range from 500 to 3000 K. The process produces carbon soot containing a melange of soluble empty cage fullerenes, soluble endohedral fullerenes, and insoluble carbon black that may contain insoluble fullerenes as well as amorphous material. Purification and isolation of the individual fullerene molecules

generally begins with the extraction of soluble fullerenes and the polyaromatic hydrocarbons that accompany fullerene generation into an organic solvent. Further purification involves chemical treatment to remove selected components and/or extensive chromatography (usually HPLC). A detailed procedure for processing the soot from gadolinium-doped graphite rods to obtain specific mono-metallic endohedrals of the type $\text{Gd}@C_{2n}$ (where $2n$ ranges from 60 to 90) has been published.¹² This study is particularly significant because it is concerned with both the insoluble but abundant endohedrals such as $\text{Gd}@C_{60}$ as well as the much more intensely studied, soluble endohedrals like $\text{Gd}@C_{82}$. Additionally, the arc process may be modified with various dopants to inhibit the formation of C_{60} and C_{70} , which are usually the prevalent fullerenes, and to facilitate the incorporation of complex clusters such as Gd_3N inside the cage.^{13,14,15,16,17} Despite efforts to improve the arc generation process, the yields of endohedral fullerenes produced remain low.

The Structures of Pristine, Gadolinium-Containing Endohedral Fullerenes. A number of gadolinium-containing endohedral fullerenes have been characterized by single crystal X-ray diffraction, which allows the cage size and isomeric structure to be identified. Crystallography also allows us to determine the location of the metal atom or atoms inside the cage. In order to obtain crystals of these highly symmetric molecules with their uniform outer surfaces, cocrystallization with $\text{Ni}(\text{OEP})$ (OEP is the dianion of octaethylporphyrin) is routinely employed.¹⁸ Although this cocrystallization procedure can produce crystals with remarkable degrees of order for the cage and the metal atoms inside, in some cases disorder in one or both of these components persists. However, usually there is a major orientation that is highly populated. In this review, the drawings and discussion are focused on these major orientations, and the reader is directed to the original publication for a description for the less populated, minor fullerene orientations.

Fullerenes Containing a Single Gadolinium Atom - Gd@C_{2v}(9)-C₈₂. Gd@C_{2v}(9)-C₈₂ is a particularly important molecule, since it is the most abundant gadolinium-containing endohedral fullerene produced by the electric arc synthesis.¹² Consequently, it can be obtained in sufficient quantities to allow functionalization to impart water solubility and utilization in a range of biomedically relevant studies (*vida infra*). Figure 3 shows a drawing of the structure of this endohedral fullerene.¹⁹ There are nine isomers of the C₈₂ cage that obey the isolated pentagon rule (IPR).²⁰ The IPR requires that each pentagon must be surrounded by five hexagons. This arrangement reduces the strain within the cage by avoiding direct pentagon-pentagon contact. The cage involved here has been identified as the C_{2v}(9)-C₈₂ isomer. The position of the metal ion inside this cage has been an issue of some controversy. Some evidence has been presented to suggest an anomalous structure with the metal atom located above a [6,6] bond along the C₂ axis of the cage, rather than beneath the hexagon at one end of the C₂ axis as found for La@C_{2v}(9)-C₈₂.^{21,22} Computations,²³ XANES spectroscopy,²⁴ and crystallographic data on the pristine and functionalized forms²⁵ of Gd@C_{2v}(9)-C₈₂ indicate that the metal ion is located largely at the normal position, beneath a hexagon and on the C₂ axis. Nevertheless, there is disorder in the gadolinium ion positions in the crystal. This disorder suggests that the metal ion is able to move freely within a portion of the fullerene cage. The EPR spectra of Gd@C_{2v}(9)-C₈₂ have been measured under a variety of conditions.²⁶ There is evidence that Gd@C_{2v}(9)-C₈₂ is paramagnetic molecule dimerizes at high concentration and low temperature in solution and in the solid state. The ground state of Gd@C_{2v}(9)-C₈₂ has a spin quantum number of $S = 3$. The spin of the internal gadolinium ($S = 7/2$) is coupled to the spin of the cage π -system ($S = 1/2$) antiferromagnetically.

Endohedral Fullerenes Containing Two Gadolinium Atoms. An endohedral fullerene with two metal atoms inside can exist as either the simple endohedral, $M_2@C_{2n}$, or as a carbide, $M_2C_2@C_{2n-2}$, with an M_2C_2 unit inside the carbon cage.²⁷ Single crystal X-ray diffraction studies are the most effective means to distinguish between these alternatives. This capability is particularly important for gadolinium-containing endohedrals, where the paramagnetism of the metal offers impediments to the use of ^{13}C NMR spectroscopy in structure determination.

An extensive series of endohedrals with the formula Gd_2C_{2n} , have been observed in arc generated carbon soot obtained from gadolinium-doped rods. The complete series from Gd_2C_{90} to Gd_2C_{106} , including two isomers of Gd_2C_{94} , have been separated by extensive HPLC, isolated, and their UV/vis spectra recorded.^{28,29}

A crystallographic study of the most rapidly eluting isomer of Gd_2C_{94} shows that it is a carbide: $Gd_2C_2@D_3(85)-C_{92}$. Its structure is shown in Figure 4. The molecule uses an IPR-obeying cage that is elongated about the C_3 axis. As the figure shows, the Gd_2C_2 unit has a butterfly shape with the C_2 unit perpendicular to the line connecting the two gadolinium atoms. However, extensive disorder in the gadolinium positions indicates that this unit is rather flexible and the dihedral angle between the two Gd_2C portions is variable. Computational studies of the other, more slowly eluting isomer of Gd_2C_{94} indicate that it does not contain a carbide unit, but rather is the simpler endohedral, $Gd_2@C_2(121)-C_{94}$.

The UV/vis/NIR spectra of endohedral fullerenes depend upon the cage size, charge and isomeric structure. Thus, $Sm_2@D_3(85)-C_{92}$ and $Gd_2(\mu-C_2)@D_3(85)-C_{92}$, both of which have been characterized crystallographically, have similar UV/vis/NIR spectra, since they contain the

$D_3(85)\text{-C}_{92}$ cage that bears a 4- charge.^{28,29} (The charge distributions are $(\text{Sm}^{2+})_2@[\text{D}_3(85)\text{-C}_{92}]^{4-}$ and $(\text{Gd}^{3+})_2(\mu\text{-C}_2)^{2-}@[\text{D}_3(85)\text{-C}_{92}]^{4-}$). The UV/vis/NIR spectra of Gd_2C_{90} and Gd_2C_{92} are nearly identical to those of $\text{Sm}_2@D_2(35)\text{-C}_{88}$ and $\text{Sm}_2@C_1(21)\text{-C}_{90}$, both of which have been characterized by X-ray crystallography.^{28,29} Thus, it appears that that Gd_2C_{90} and Gd_2C_{92} are the carbides $\text{Gd}_2\text{C}_2@D_2(35)\text{-C}_{88}$ and $\text{Gd}_2\text{C}_2@C_1(21)\text{-C}_{90}$.

A crystallographic study of Gd_2C_{86} reveals that it, too, is a carbide: $\text{Gd}_2\text{C}_2@C_1(51383)\text{-C}_{84}$.³⁰ Its structure is shown in Figure 5. Unlike the endohedral fullerenes discussed previously, this example does not obey the IPR. Rather it has a cage with one position where two pentagons abut to form a pentalene-like unit. In Figure 5, this unit is highlighted in red. One of the gadolinium ions is bonded to the fold of the pentalene unit, while the other resides near a hexagon at the opposite side of the cage. The Gd_2C_2 unit again has a butterfly shape, but an asymmetric one with the carbide significantly closer to the gadolinium atom nearest the hexagon.


Computational studies for $\text{Gd}_2@C_{98}$, which has yet to be isolated and structurally identified, indicate that the non-IPR species $\text{Gd}_2@C_1(168785)\text{-C}_{98}$ is the most thermodynamically stable structure over the temperature range 200 to 2000 K.³¹ Additionally, this isomer has a large SOMO-LUMO gap. Unfortunately, this study did not comment upon the relative stabilities of the $\text{Gd}_2@C_{98}$ and the $\text{Gd}_2\text{C}_2@C_{96}$ isomers. It is, however, noteworthy that this computation predicts stability for a rather large non-IPR cage. Earlier computational studies had suggested that the occurrence of non-IPR endohedrals would be limited to cage sizes in smaller than C_{86} .³²

The azafullerene, $\text{Gd}_2@C_{79}\text{N}$, which also contains two gadolinium atoms, has been prepared and characterized by UV/vis, Raman and electron spin resonance (ESR) spectroscopy as well as through computations.³³ The ESR studies have shown that the spin resides on the

interior of the molecule with the unpaired electron spin density localized on the internal diatomic gadolinium cluster and not on the heterofullerene cage. From these EPR studies it was deduced that the spin ($S = 1/2$) of the nitrogen atom is coupled ferromagnetically with the spins of the two gadoliniums ($S = 7/2$) to yield a molecule with overall $S = 15/2$. Other endohedrals of this type have also been prepared including: $\text{La}_2@C_{79}\text{N}$,³⁴ $\text{Y}_2@C_{79}\text{N}$ and $\text{Tb}_2@C_{79}\text{N}$.³⁵ The structure of $\text{Tb}_2@C_{79}\text{N}$ has been determined crystallographically and serves as a model for that of $\text{Gd}_2@C_{79}\text{N}$. The structure of $\text{Tb}_2@C_{79}\text{N}$ is shown in Figure 6. The molecule utilizes a cage with the same symmetry as $I_h\text{-C}_{80}$, but one of the carbon atoms is replaced by a nitrogen atom. In the crystal, the position of that nitrogen atom is, not unexpectedly, disordered. Nevertheless, the overall cage geometry is well established. Inside the cage, the two terbium atoms are widely separated by 3.9020(10) Å, but computational studies suggest that there is a bonding interaction between these atoms and that the nitrogen atom is centrally located between two terbium atoms on a junction of two hexagons and a pentagon.

The $\text{Gd}_3\text{N}@C_{2n}$ ($2n = 78$ to 88) Family of Endohedral Fullerenes. When fullerenes are produced by the arc process in the presence of a nitrogen source (*e. g.* N_2 , NH_3), a new series of endohedrals containing the M_3N unit are formed.¹³⁻¹⁶ Figure 7 shows the mass spectrum obtained from the soluble extract formed from conducting the arc synthesis with gadolinium-doped graphite electrodes.³⁶ As the figure shows, the complete series of endohedrals from $\text{Gd}_3\text{N}@C_{78}$ to $\text{Gd}_3\text{N}@C_{88}$ is formed. The size of the metal involved in this process determines the size of cages formed. Thus, with the smaller metal, scandium, the series produced ($\text{Sc}_3\text{N}@C_{68}$, $\text{Sc}_3\text{N}@C_{78}$ and $\text{Sc}_3\text{N}@C_{80}$) includes smaller cages,³⁷ while with a larger metal, lanthanum, a series with larger cages, $\text{La}_3\text{N}@C_{88}$ to $\text{La}_3\text{N}@C_{110}$, is formed.³⁸ We are fortunate

to have extensive crystallographic data for the $\text{Gd}_3\text{N}@C_{78}$ to $\text{Gd}_3\text{N}@C_{88}$ series.

It is informative to compare the structures of $\text{M}_3\text{N}@C_{78}$, where $\text{M} = \text{Sc}$ and Gd . The two compounds have markedly different colors. In solution, the scandium compound is green, while the gadolinium analog is brown.³⁹ Since the colors and electronic spectra reflect the nature of the fullerene cage present, it seems that the two compounds must have different structures. For the C_{78} cage there are five isomers that obey the IPR. Figure 8 shows the structure of $\text{Sc}_3\text{N}@D_{3h}(5)-C_{78}$.^{40,41,42} The cage is one that obeys the IPR. The Sc_3N unit resides in the horizontal mirror plane of the fullerene and the entire molecule has D_{3h} symmetry. In contrast the gadolinium analog utilizes a non-IPR cage. Figure 9 shows the structure of this compound, $\text{Gd}_3\text{N}@C_2(22010)-C_{78}$.³⁹  $\text{Sc}_3\text{N}@D_{3h}(5)-C_{78}$, which follows the IPR, $\text{Gd}_3\text{N}@C_2(22010)-C_{78}$ uses one of the 24105 isomers that do not follow the IPR. As Figure 9 shows, there are two sites where pentagon pairs abut in this cage. These are highlighted in red in the figure. There is some disorder in the positions of the gadolinium ions within the cage. However, in the major site, two of the three gadolinium ions are located within the folds of these pentalene units. The other gadolinium ion is situated beneath a hexagonal ring of the fullerene cage. Computational studies show that $\text{Gd}_3\text{N}@C_2(22010)-C_{78}$ is the most stable isomer of over a wide temperature range, 0 to 6500 K.⁴³

The next member of the series, $\text{Gd}_3\text{N}@I_h-C_{80}$, whose structure is shown in Figure 10, utilizes the popular, highly symmetric I_h-C_{80} cage, which obeys the IPR.^{44,45} Many other endohedrals of the $\text{M}_3\text{N}@C_{80}$ type also use this cage.⁴⁶ The remarkable feature of $\text{Gd}_3\text{N}@I_h-C_{80}$ is the pyramidalization of the Gd_3N unit on the inside. The central nitrogen atom is disordered over two sites with fractional occupancies of 0.309(9) for N1A and 0.191(9) for N1B. N1A is 0.522(8) Å away from the plane of the three gadolinium ions, while at the minor site, N1B is

0.463 Å from the Gd₃ plane. In contrast, many other endohedrals of the M₃N@I_h-C₈₀ type, like Sc₃N@I_h-C₈₀ and Lu₃N@I_h-C₈₀, have planar M₃N cores.⁴⁷ The magnetic properties of Gd₃N@I_h-C₈₀ have been reported.^{48,49} At low temperatures, the spins of the gadolinium ions are ferromagnetically aligned, while at high temperatures these spins are uncorrelated.⁵⁰ The Raman and inelastic electron tunneling spectra of Gd₃N@I_h-C₈₀ and related endohedrals have been reported.⁵¹

In addition to Gd₃N@I_h-C₈₀, the mixed metal endohedrals Gd₂ScN@I_h-C₈₀, GdSc₂N@I_h-C₈₀, Gd₂ScN@D_{5h}-C₈₀, and GdSc₂N@D_{5h}-C₈₀ have been prepared and isolated by using a mixture of Gd₂O₃ and Sc₂O₃ to dope the graphite rods used in the initial fullerene generation.^{52,53,54,55} These molecules have been characterized by UV/vis, infrared and Raman spectroscopy and by DFT calculations. Additionally, Gd₂ScN@I_h-C₈₀ and GdSc₂N@I_h-C₈₀ have been characterized crystallographically.⁵² The structures of these two endohedrals are shown in Figures 11 and 12. The Gd₂Sc and GdSc₂ units in these two structures are planar and are situated so that their planes are nearly perpendicular to the plane of the Ni(OEP) molecules in the respective cocrystals. Moreover, for such mixed-metal endohedrals of the type, M₂M'N@I_h-C₈₀, the metal atoms with lowest atomic number are situated nearer the Ni(OEP) molecule than are the metal atoms with higher atomic number. The causes for this orientational preference need further study. While both Sc₃N@I_h-C₈₀ and Sc₃N@D_{5h}-C₈₀ have been isolated and structurally characterized,^{13,56} it is curious that no one has reported the existence of “Gd₃N@D_{5h}-C₈₀”.

There are 9 IPR and 39709 non-IPR isomers of C₈₂. One isomer of Gd₃N@C₈₂ has been isolated and purified.⁵⁷ Its structure is shown in Figure 13. Gd₃N@C_s(39663)-C₈₂, contains an unusual, egg-shaped fullerene that does not obey the IPR. There is one site in this molecule where two pentagons abut. That portion is highlighted in red in Figure 13. Notice that one of

the three gadolinium ions resides within the fold of this pentalene unit. The Gd_3N unit within the cage is planar. Computational studies have shown the experimentally observed isomer, $Gd_3N@C_s(39663)-C_{82}$, only becomes predominant at synthesis temperatures above 3400 K.⁵⁸ Below that temperature, another non-IPR isomer with a single pair of abutting pentagons, $Gd_3N@C_s(39705)-C_{82}$, is prevalent.

For the C_{84} cage there are 24 IPR and 51568 non-IPR isomers. Three isomers with the composition $Gd_3N@C_{84}$ have been separated and purified.⁵⁹ A sufficient quantity of the most abundant of these has been obtained to allow crystallization and examination by X-ray crystallography. The structure of this isomer, $Gd_3N@C_s(51365)-C_{84}$, is shown in Figure 14. This molecule is another egg-shaped endohedral with one position where a pentalene unit is formed by two neighboring five-membered rings. Again, one of the gadolinium ions is located near that pentalene portion of the cage and the Gd_3N unit is planar. Two isomers of $Tb_3N@C_{84}$ and two isomers of $Tm_3N@C_{84}$ have also been isolated.^{57,60} In both cases crystallographic studies have shown that the most abundant isomer for Tb and Tm utilizes the same cage as found in $Gd_3N@C_s(51365)-C_{84}$. Thus, in these cases the identity of the internal metal ions does not produce a change in cage geometry for the most abundant endohedral.

The structures of $Gd_3N@C_s(39663)-C_{82}$ and $Gd_3N@C_s(51365)-C_{84}$ shown in Figures 13 and 14 are rather similar. Both utilize non-IPR, egg-shaped cages that have one pair of fused pentagons. The shapes of these cages are compared in Figure 15. Because of the unusual shapes of these non-IPR cages and the placement of metal ions within the nose formed by the pentalene portion, Dorn and coworkers have predicted that these egg-shaped endohedrals will have significant dipole moments that are much larger than those found for endohedral fullerenes that lack pentalene moieties.⁶¹

Finally with the C_{86} cage, we reach a cage size that will allow a planar Gd_3N unit to fit inside a cage that obeys the IPR. Two orthogonal views of the crystallographically determined structure of $Gd_3N@D_3(17)-C_{86}$ are shown in Figure 16.⁶² As the figure shows, the chiral cage is somewhat squashed along the three-fold axis and the Gd_3N unit fits into the widest part of the cage. Crystallographic studies of $Tb_3N@D_3(17)-C_{86}$ reveal that it possesses a similar structure.⁶³

No crystallographic data are available for $Gd_3N@C_{88}$. However, the structure of the related molecule, $Tb_3N@D_2(35)-C_{88}$, has been determined by single crystal X-ray diffraction.⁵⁹ Its structure is shown in Figure 17. The electronic spectra of the only known isomer of $Gd_3N@C_{88}$ and that of $Tb_3N@D_2(35)-C_{88}$ are similar. Consequently, it is likely that these two molecules utilize the same cage isomer. Likewise, $Tm_3N@D_2(35)-C_{88}$ has recently been characterized crystallographically.⁶⁴ Additionally, density functional calculations indicate that the lowest energy isomers of $M_3N@C_{88}$ for $M = Gd$ and Lu are $Gd_3N@D_2(35)-C_{88}$ and $Lu_3N@D_2(35)-C_{88}$.⁶⁵ However, for $La_3N@C_{88}$ a different, C_s symmetric structure is predicted for the cage.

In considering the $Gd_3N@C_{78}$ to $Gd_3N@C_{88}$ family of endohedrals, it is striking to see that half of the members do not obey the IPR. Only when the cage size reaches $Gd_3N@C_{86}$ do we find a planar Gd_3N core accommodated within an IPR cage. For small cage sizes these fullerenes utilize either a non-IPR cage (as found for $Gd_3N@C_2(22010)-C_{78}$, $Gd_3N@C_s(39663)-C_{82}$, and $Gd_3N@C_s(51365)-C_{84}$) or a pyramidalized Gd_3N core (as seen in $Gd_3N@I_h-C_{80}$).

Electrochemical Studies of Gadolinium-Containing Endohedrals. Endohedral fullerenes and empty cage fullerenes undergo step-wise, one-electron oxidation and reduction. These redox characteristics are not exploited in the use of gadolinium-containing endohedrals as MRI agents, but they are an important, intrinsic property of these cage molecules. Table 1 contains information

obtained from cyclic voltammetric studies of several gadolinium-containing endohedrals of the type $\text{Gd}_3\text{N}@C_{2n}$. The data reveal that these endohedrals generally undergo irreversible reductions for which the E_p (reduction peak potential) values are given. One, two or three reduction waves are observed for these compounds. Additionally, one or two reversible, one-electron oxidations occur for which the $E_{1/2}$ values are given in the Table. It is interesting to note that, within the series, $\text{Gd}_3\text{N}@I_h\text{-C}_{80}$, $\text{Gd}_3\text{N}@C_s(51365)\text{-C}_{84}$, and $\text{Gd}_3\text{N}@D_2(35)\text{-C}_{88}$, increasing cage size is accompanied by an decrease in the value of ΔE_{gap} . ΔE_{gap} is the difference between the first oxidation potential and the first reduction potential and is related to the HOMO-LUMO gap. This decrease in ΔE_{gap} is largely due to the decrease in the $E_{1/2}$ value for oxidation, whereas the potential for the first reduction is little changed within this series. It is also interesting to notice that replacement of gadolinium by scandium in these endohedrals produces only rather minor changes in the various redox potentials.

External Functionalization Gadolinium-Containing Endohedrals.

Work on functionalization of gadolinium-containing endohedrals can be classified into two groups: studies that focus on examining the reactivity of these novel compounds and produce well-defined adducts and studies designed to impart water solubility to the cage for use in work of biological and medicinal relevance. The latter frequently seems sacrilegious to those of us who treasure isomerically pure samples of endohedrals for structural characterization, since the process of imparting water solubility usually results in the formation of a mixture of adducts with different numbers of addends appended to the fullerene outer surface. Nevertheless, such functionalization is effective in imparting water solubility to what is otherwise a hydrophobic molecule.

There are only a few studies that have been performed to prepare well defined mono- and di-adducts of the gadolinium endohedrals. When a toluene solution of $\text{Gd}@C_{2v}(9)\text{-C}_{82}$ and 2-

adamantane-2,3-[3H]-diazirine (ADN₂) is photolyzed with a high pressure mercury lamp, the mono-adduct Gd@C_{2v}(9)-C₈₂(Ad) (Ad = C₁₀H₁₄) is formed in 95 % yield.⁶⁶ The product has been characterized by single crystal X-ray diffraction. As seen in Figure 18, adduct formation is accompanied by the rupture of the C1A-C2A bond (a 6:6 ring junction) within the fullerene cage. The gadolinium is situated close to the site of addition but at a site comparable to that found in the unfunctionalized version of this molecule, which is shown in Figure 3.

The reactivity of the Gd₃N@I_h-C₈₀, Gd₃N@C_s(51365)-C₈₄, and Gd₃N@D₂(35)-C₈₈ in the Bingel cyclopropanation reaction with bromomalonate shows a remarkable size effect.^{67,68} With Gd₃N@I_h-C₈₀, both a mono and a di-adduct are formed. Under similar conditions with Gd₃N@C_s(51365)-C₈₄ only a monadduct was found, but with Gd₃N@D₂(35)-C₈₈ no evidence for adduct formation was found. Thus, the larger the cage, the less reactive that endohedral is for Bingel adduct formation. Moreover, the non-IPR nature of Gd₃N@C_s(51365)-C₈₄ does not appear to convey any unusually high reactivity to that molecule.

Due to their potential utility, much more attention has been given to devising means to make gadolinium-containing endohedrals water soluble for use as MRI contrast agents. The two prominent methods of solubilization involve either polyhydroxylation, in which multiple OH groups are added to the cage surface, or utilization of the Bingel reaction, a cyclopropanation reaction that leads to the addition of several C(COOH)₂ groups to the fullerene. In both cases, it must be assumed that adducts are formed with a variety of addition patterns that produce a complex mixture of regioisomers.

The initial work on water solubilization of gadolinium-containing endohedrals was performed by Shinohara and coworkers.^{69,70} They treated the relatively abundant Gd@C_{2v}-C₈₂ in toluene solution with a 50 wt % solution of sodium hydroxide in water with either 15-crown-5 or

tetrabutylammonium hydroxide as a phase transfer catalyst at room temperature to form a polyhydroxylated species ($\text{Gd}@C_{2v}\text{-C}_{82}(\text{OH})_n$ with $n \sim 40$) that was purified by dialysis. Other water-soluble forms of $\text{Gd}@C_{2v}\text{-C}_{82}$ have been prepared. For example, the related amino acid functionalized compound, $\text{Gd}@C_{2v}\text{-C}_{82}\text{O}_m(\text{OH})_n\text{-}(\text{NHCH}_2\text{CH}_2\text{COOH})_l$ ($m \sim 6$, $n \sim 16$ and $l \sim 8$), has been synthesized.⁷¹ Water soluble $\text{Gd}@C_{2v}\text{-C}_{82}\text{O}_2(\text{OH})_{16}(\text{C}(\text{PO}_3\text{Et}_2)_2)_{10}$ was obtained by a Bingel-type reaction by treating a toluene solution of $\text{Gd}@C_{2v}\text{-C}_{82}$ and tetraethyl methylenediphosphonate with sodium hydride.⁷²

Bolskar *et al* developed an ingenious way to functionalize and solubilize the relatively abundant, but insoluble, $\text{Gd}@C_{60}$.⁷³ They prepared an enriched sample of $\text{Gd}@C_{60}$ through a series of solvent extractions (to remove soluble fullerenes) and sublimations. Subsequently, they functionalized the $\text{Gd}@C_{60}$ through the reaction with diethyl bromomalonate and sodium or potassium hydride to form Bingel adducts, $\text{Gd}@C_{60}[\text{C}(\text{COOCH}_2\text{CH}_3)_2]_x$ ($x \sim 10$). To obtain water soluble material, $\text{Gd}@C_{60}[\text{C}(\text{COOCH}_2\text{CH}_3)_2]_x$ was converted into the corresponding acid $\text{Gd}@C_{60}[\text{C}(\text{COOH})_2]_x$. Additionally, a procedure for the polyhydroxylation of $\text{Gd}@C_{60}$ has been devised.⁷⁴

Both the polyhydroxylated and polycarboxylated types of endohedral fullerenes are prone to aggregation in aqueous solution.^{75,76} These clusters have sizes in the 30 and 90 nm range and are likely to be responsible for the activity of these MRI contrast agents. This aggregation is sensitive to the presence of various salts in solution with phosphate exhibiting a large effect in disrupting the aggregates.⁷⁷

Several water soluble forms of $\text{Gd}_3\text{N}@I_h\text{-C}_{80}$ have been prepared by Dorn and others. $\text{Gd}_3\text{N}@I_h\text{-C}_{80}(\text{OH})_x(\text{CH}_2\text{CH}_2\text{COOM})_y$ was obtained by treatment of $\text{Gd}_3\text{N}@I_h\text{-C}_{80}$ with succinic acid acyl peroxide.⁷⁸ Procedures for converting $\text{Gd}_3\text{N}@I_h\text{-C}_{80}$ into the water-soluble pegylated and

polyhydroxylated products, $\text{Gd}_3\text{N}@I_h\text{-C}_{80}[\text{DiPEG5000}(\text{OH})_x]$ and $\text{Gd}_3\text{N}@I_h\text{-C}_{80}[\text{DiPEG}(\text{OH})_x]$, have also been published.^{79,80} A proposed structure for $\text{Gd}_3\text{N}@I_h\text{-C}_{80}[\text{DiPEG}(\text{OH})_x]$ is shown in Figure 19. $\text{Gd}_3\text{N}@I_h\text{-C}_{80}$ has also been converted into $\text{Gd}_3\text{N}@I_h\text{-C}_{80}\text{-}[\text{N}(\text{OH})(\text{CH}_2\text{CH}_2\text{O})_n\text{CH}_3]_x$ where n is 1, 3, or 6 and x ranges from 10 to 22.⁸¹ The mixed metal fullerenes, $\text{Sc}_x\text{Gd}_{3-x}\text{N}@I_h\text{-C}_{80}$ ($x = 1$ or 2), have also been functionalized to form $\text{Sc}_x\text{Gd}_{3-x}\text{N}@I_h\text{-C}_{80}\text{O}_m(\text{OH})_n$ with $m \approx 12$; $n \approx 26$.⁸²

Applications of Gadolinium-Containing Endohedrals.

Considerable attention has been given to the properties of gadolinium-containing fullerenes as MRI contrast agents, ever since Shinohara and coworkers demonstrated that the relaxivity obtained from $\text{Gd}@C_{2v}\text{-C}_{82}(\text{OH})_n$ was about twenty-fold greater than that of the commercial MRI contrast agent, Magnevist.⁶⁹ Most of the water-soluble versions of gadolinium-containing fullerenes described in the preceding section have been examined as MRI contrast agents and found to show considerable activity in that regard. For example, water soluble $\text{Gd}@C_{2v}\text{-C}_{82}\text{O}_2(\text{OH})_{16}(\text{C}(\text{PO}_3\text{Et}_2)_2)_{10}$ exhibited a higher longitudinal water proton relaxivity ($37.0 \text{ mM}^{-1} \text{ s}^{-1}$) than the conventional, chelated gadolinium complex in Omniscan ($5.7 \text{ mM}^{-1} \text{ s}^{-1}$).⁷²

Additional studies have been conducted to better understand the relaxation phenomena involved with these new relaxation agents. The effects of pH and salt concentration on aggregation in aqueous solution are important factors that need to be carefully controlled when one is comparing the efficacy of different contrast agents. For unaggregated monomers, a mechanism involving proton exchange between OH or COOH sites on the fullerene with bulk water is important to the relaxivity.⁸³ For solutions containing aggregates of the hydroxylated or

carboxylated fullerenes, there are water molecules located in the interstices of the aggregates. These water molecules can exchange rapidly with bulk water to contribute to the proton relaxation.

Recent developments in the use of gadolinium-containing fullerenes as MRI contrast agents have focused on targeting these compounds to specific biological targets. Thus, the $Gd_3N@I_h-C_{80}$ platform has been solubilized and conjugated with specific peptides of the IL-13 class to make reagents that target and image glial tumors.⁸⁴ Similarly, fullerenes of the type $Gd_xSc_{3-x}N@I_h-C_{80}$ have been covalently linked to an SV40 T-antigen and that antigen connected by a disulfide connector to a peptide that would promote passage across cell membranes.⁸⁵

Additionally, a solubilized form of has been used for neutron capture therapy since both ^{155}Gd (14.8% natural abundance) and ^{157}Gd (15.7 na) have high neutron capture cross sections.⁸⁶

Acknowledgments. We thank our collaborators, Profs. H. C. Dorn, S. Stevenson, L. Echegoyen, Z. Liu, and H. Wang, for providing the endohedral fullerenes for crystallographic study and the National Science Foundation [Grants CHE-1305125 and CHE-1011760 to ALB and MMO] for support.

References

- 1 P. Caravan, J. J. Ellison, T. J. McMurry and R. B. Lauffer, *Chem. Rev.*, 1999, **99**, 2293.
- 2 M. Bottrill, L. Kwok and N. J. Long, *Chem. Soc. Rev.*, 2006, **35**, 557–571.
- 3 J. G. Penfield and R. F. Reilly, Jr., *Nat. Clinical Practice Nephrol.*, 2007, **3**, 654–668.
- 4 S. Aime, M. Botta, Z. Garda, B. E. Kucera, G. Tircso, V. G. Young and M. Woods, *Inorg. Chem.*, 2011, **50**, 7955–7965.

-
- 5 T. Grobner, *Nephrol. Dial. Transplant.*, 2006, **21**, 1104–1108.
- 6 P. Marckmann, L. Skov, K. Rossen, A. Dupont, M. B. Damholt, J. G. Heaf and H. S. Thomsen, *J. Am. Soc. Nephrol.* 2006, **17**, 2359–2362.
- 7 X. Lu, T. Akasaka, S. Nagase, *Chem. Commun.*, 2011, **47**, 5942-5957.
- 8 A. Rodriguez-Forteza, A. L. Balch and J. M. Poblet, *Chem. Soc. Rev.*, 2011, **40**, 3551-3563.
- 9 A. A. Popov, S.-F. Yang and L. Dunsch, *Chem. Rev.*, 2013, **113**, 5989–6113.
- 10 J. R. Heath, S. C. O'Brien, Q. Zhang, Y. Liu, R. F. Curl, H. W. Kroto, F. K. Tittel and R. E. Smalley, *J. Am. Chem. Soc.*, 1985, **107**, 1179-1180.
- 11 W. Krätschmer, L. D. Lamb, K. Fostiropoulos and D. R. Huffman, *Nature*, **1990**, *347*, 354-358.
- 12 J. W. Raebiger and R. D. Bolskar, *J. Phys. Chem. C*, 2008, **112**, 6605-6612.
- 13 S. Stevenson, G. Rice, T. Glass, K. Harich, F. Cromer, M. R. Jordan, J. Craft, E. Hadju, R. Bible, M. M. Olmstead, K. Maitra, A. J. Fisher, A. L. Balch and H. C. Dorn, *Nature*, 1999, **401**, 55 – 57.
- 14 L. Dunsch, M. Krause, J. Noack and P. Georgi, *J. Phys. Chem. Solids*, 2004, **65**, 309–315.
- 15 M. Jiao, W. Zhang, Y. Xu, T. Wei, C. Chen, F. Liu and S.-F. Yang, *Chem.-Eur. J.*, 2012, **18**, 2666-2673.
- 16 S. Stevenson, M. C. Thompson, H. L. Coumbe, M. A. Mackey, C. E. Coumbe and J. P. Phillips, *J. Am. Chem. Soc.*, 2007, **129**, 16257-16262.
- 17 H. Yang, H. X. Jin, H. Zhen, Z. M. Wang, Z. L. Liu, C. M. Beavers, B. Q. Mercado, M. M. Olmstead and A. L. Balch, *J. Am. Chem. Soc.*, 2011, **133**, 6299-6306.

-
- 18 M. M. Olmstead, D. A. Costa, K. Maitra, B. C. Noll, S. L. Phillips, P. M. Van Calcar and A. L. Balch, *J. Am. Chem. Soc.*, 1999, **121**, 7090-7097.
- 19 M. Suzuki, X. Lu, S. Sato, H. Nikawa, N. Mizorogi, Z. Slanina, T. Tsuchiya, S. Nagase and T. Akasaka, *Inorg. Chem.*, 2012, **51**, 5270–5273.
- 20 P. W. Fowler and D. E. Manolopoulos, *An Atlas of Fullerenes*, Clarendon, Oxford, 1995.
- 21 N. Mizorogi and S. Nagase, *Chem. Phys. Lett.*, 2006, **431**, 110–112.
- 22 L. Liu, B. Gao, W. Chu, D. Chen, T. Hu, C. Wang, L. Dunsch, A. Marcelli, Y. Luo and Z. Wu, *Chem. Commun.*, 2008, 474–476.
- 23 E. Nishibori, K. Iwata, M. Sakata, M. Takata, H. Tanaka, H. Kato and H. Shinohara, *Phys. Rev. B*, 2004, **69**, 113412.
- 24 B.-Y. Sun, T. Sugai, E. Nishibori, K. Iwata, M. Sakata, M. Takata and H. Shinohara, *Angew. Chem., Int. Ed.*, 2005, **44**, 4568–4571.
- 25 T. Akasaka, T. Kono, Y. Takematsu, H. Nikawa, T. Nakahodo, T. Wakahara, M. O. Ishitsuka, T. Tsuchiya, Y. Maeda, M. T. H. Liu, K. Yoza, T. Kato, K. Yamamoto, N. Mizorogi, Z. Slanina and S. Nagase, *J. Am. Chem. Soc.*, 2008, **130**, 12840–12841.
- 26 K. Furukawa, S. Okubo, H. Kato, H. Shinohara and T. Kato, *J. Phys. Chem. A*, 2003, **107**, 10933-10937.
- 27 X. Lu, T. Akasaka and S. Nagase, *Accounts Chem. Res.*, 2013, **46**, 1627-1635.
- 28 H. Yang, C. Lu, Z. Liu, H. Jin, Y. Che, M. M. Olmstead and A. L. Balch, *J. Am. Chem. Soc.*, 2008, **130**, 17296-17300.
- 29 H. Yang, H. Jin, B. Hong, Z. Liu, C. M. Beavers, H. Zhen, Z. Wang, B. Q. Mercado, M. M. Olmstead and A. L. Balch, *J. Am. Chem. Soc.*, 2011, **133**, 16911-16919.

- 30 J. Zhang, F. L. Bowles, D. W. Bearden, W. K. Ray, T. Fuhrer, Y. Ye, C. Dixon, K. Harich, R. F. Helm, M. M. Olmstead, A. L. Balch and H. C. Dorn, *Nat. Chem.*, 2013, **5**, 880-885.
- 31 X. Zhao, W.-Y. Gao, T. Yang, J.-J. Zheng, L.-S. Li, L. He, R.-J. Cao and S. Nagase, *Inorg. Chem.*, 2012, **51**, 2039–2045.
- 32 N. Alegret, M. Mulet-Gas, X. Aparicio-Anglés, A. Rodríguez-Fortea and J. M. Poblet, *C. R. Chimie*, 2012, **15**, 152-158.
- 33 W. Fu, J. Zhang, T. Fuhrer, H. Champion, K. Furukawa, T. Kato, J. E. Mahaney, B. G. Burke, K. A. Williams, K. Walker, C. Dixon, J. Ge, C. Shu, K. Harich and H. C. Dorn, *J. Am. Chem. Soc.*, 2011, **133**, 9741–9750.
- 34 T. Akasaka, S. Okubo, T. Wakahara, K. Yamamoto, K. Kobayashi, S. Nagase, T. Kato, M. Kako, Y. Nakadaira, Y. Kitayama, and K. Matsuura, *Chem. Lett.*, 1999, 945.
- 35 T. Zuo, L. Xu, C. M. Beavers, M. M. Olmstead, W. Fu, D. Crawford, A. L. Balch and H. C. Dorn, *J. Am. Chem. Soc.*, 2008, **130**, 12992-12997.
- 36 M. N. Chaur, F. Melin, B. Elliott, A. J. Athans, K. Walker, B. C. Holloway and L. Echegoyen *J. Am. Chem. Soc.*, 2007, **129**, 14826-14829.
- 37 M. M. Olmstead, A. de Bettencourt-Dias, J. C. Duchamp, S. Stevenson, Da. Marciu, H. C. Dorn and A. L. Balch, *Angew. Chem. Int. Ed.*, 2001, **40**, 1223-1225.
- 38 M. N. Chaur, F. Melin, J. Ashby, B. Elliott, A. Kumbhar, A. M. Rao and L. Echegoyen, *Chem. Eur. J.*, 2008, **14**, 8213–8219.
- 39 C. M. Beavers, M. N. Chaur, M. M. Olmstead, L. Echegoyen and A. L. Balch, *J. Am. Chem. Soc.*, 2009, **131**, 11519–11524.

- 40 M. M. Olmstead, A. de Bettencourt-Dias, J. C. Duchamp, S. Stevenson, D. Marciu, H. C. Dorn and A. L. Balch, *Angew. Chem., Int. Ed.*, 2001, **40**, 1223-1225.
- 41 J. M. Campanera, C. Bo, M. M. Olmstead, A. L. Balch and J. M. Poblet, *J. Phys. Chem. A*, 2002, **106**, 12356-12364.
- 42 B. Q. Mercado, M. N. Chaur, L. Echegoyen, J. A. Gharamaleki, M. M. Olmstead and A. L. Balch, *Polyhedron*, 2013, **58**, 129–133.
- 43 T. Yang, X. Zhao, L.-S. Li, J.-J. Zheng and W.-Y. Gao, *ChemPhysChem*, 2012, **13**, 449 – 452.
- 44 S. Stevenson, J. P. Phillips, J. E. Reid, M. M. Olmstead, S. P. Rath and A. L. Balch, *Chem. Commun.*, 2004, 2814-2815.
- 45 M. Krause and L. Dunsch, *Angew. Chem. Int. Ed.*, 2005, **44**, 1557 –1560.
- 46 L. Dunsch and S.-F. Yang, *Small*, 2007, **3**, 1298 – 1320.
- 47 S. Stevenson, H. M. Lee, M. M. Olmstead, C. Kozikowski, P. Stevenson and A. L. Balch. *Chem. Eur. J.*, 2002, **8**, 4528-4535.
- 48 J. Lu, R. F. Sabirianov, W. N. Mei, Y. Gao, C.-G. Duan, and X. Zeng, *J. Phys. Chem. B*, 2006, **110**, 23637-23640.
- 49 L. Chen, E. E. Carpenter, C. S. Hellberg, H. C. Dorn, M. Shultz, W. Wernsdorfer and I. Chiorescu, *J. Appl. Phys.*, 2011, **109**, 07B101.
- 50 B. Náfádi, Á. Anatal, Á. Pászor, L. Forró, L. F. Kiss, T. Fehér, É. Kováts, S. Pekkern and Jánossy, *J. Phys. Chem. Lett.* 2012, **3**, 3291–3296.
- 51 B. G. Burke, J. Chan, K. A. Williams, J. Ge, C. Shu, W. Fu, H. C. Dorn, J. G. Kushmerick, A. A. Puretzky and D. B. Geohegan, *Phys. Rev. B*, 2010, **81**, 115423.

- 52 S. Stevenson, C. J. Chancellor, H. M. Lee, M. M. Olmstead and A. L. Balch, *Inorg. Chem.*, 2008, **47**, 1420-1427.
- 53 S.-F. Yang, A. Popov, M. Kalbac and L. Dunsch, *Chem. Eur. J.*, 2008, **14**, 2084 – 2092.
- 54 S.-F. Yang, M. Kalbac, A. Popov and L. Dunsch, *ChemPhysChem*, 2006, **7**, 1990-1995.
- 55 A. L. Svitova, A. A. Popov and L. Dunsch, *Inorg. Chem.* 2013, **52**, 3368–3380.
- 56 T. Cai, L. Xu, M. R. Anderson, Z. Ge, T. Zuo, X. Wang, M. M. Olmstead, A. L. Balch, H. W. Gibson and H. C. Dorn, *J. Am. Chem. Soc.*, 2006, **128**, 8581-8589.
- 57 B. Q. Mercado, C. M. Beavers, M. M. Olmstead, M. N. Chaur, K. Walker, B. C. Holloway, L. Echegoyen and A.L. Balch, *J. Am. Chem. Soc.*, 2008, **130**, 7854–7855.
- 58 M. Mulet-Gas, A. Rodríguez-Forteza, L. Echegoyen and J. M. Poblet, *Inorg. Chem.*, 2013, **52**, 1954–1959.
- 59 T. Zuo, K. Walker, M. M. Olmstead, F. Melin, B. C. Holloway, L. Echegoyen, H. C. Dorn, M. N. Chaur, C. J. Chancellor, C. M. Beavers, A. L. Balch and A. J. Athans, *Chem. Commun.*, 2008, 1067-1069.
- 60 C. M. Beavers, T. Zuo, J. C. Duchamp, K. Harich, H. C. Dorn, M. M. Olmstead and A. L. Balch, *J. Am. Chem. Soc.*, 2006, **128**, 11352-11353.
- 61 J. Zhang, D. W. Bearden, T. Fuhrer, L. Xu, W. Fu, T. Zuo and H. C. Dorn, *J. Am. Chem. Soc.* 2013, **135**, 3351–3354.
- 62 M. N. Chaur, X. Aparicio-Anglés, B. Q. Mercado, B. Elliott, A. Rodríguez-Forteza, A. Clotet, M. M. Olmstead, A. L. Balch, J. M. Poblet and L. Echegoyen, *J. Phys. Chem. C*, 2010, **114**, 13003–13009.
- 63 T. Zuo, C. M. Beavers, J. C. Duchamp, A. Campbell, H. C. Dorn, M. M. Olmstead and A. L. Balch, *J. Am. Chem. Soc.*, 2007, **129**, 2035–2043.

-
- 64 T. Zuo, H. C. Dorn, C. M. Beavers, M. M. Olmstead and A. L. Balch, *Fullerenes, Nanotubes, Carbon Nanostruct.* 2014, DOI:10.1080/1536383X.2013.812641.
- 65 L. Xu, S.-F. Li, L.-H. Gan, C.-Y. Shu and C.-R. Wang, *Chem. Phys. Lett.*, 2012, **521**, 81–85.
- 66 T. Akasaka, T. Kono, Y. Takematsu, H. Nikawa, T. Nakahodo, T. Wakahara, M. O. Ishitsuka, T. Tsuchiya, Y. Maeda, M. T. H. Liu, K. Yoza, T. Kato, K. Yamamoto, N. Mizorogi, Z. Slanina and S. Nagase, *J. Am. Chem. Soc.* 2008, **130**, 12840–12841.
- 67 C. Bingel, *Chem. Ber.*, 1993, **126**, 1957-1959.
- 68 M. N. Chaur, F. Melin, A. J. Athans, B. Elliott, K. Walker, B. C. Holloway and L. Echegoyen, *Chem. Commun.*, 2008, 2665–2667.
- 69 M. Mikawa, H. Kato, M. Okumura, M. Narazaki, Y. Kanazawa, N. Miwa and H. Shinohara, *Bioconjugate Chem.*, 2001, **12**, 510.
- 70 H. Kato, Y. Kanazawa, M. Okumura, A. Taninaka, T. Yokawa and H. Shinohara, *J. Am. Chem. Soc.*, 2003, **125**, 4391-4397.
- 71 C. Y. Shu, L. H. Gan, C. R. Wang, X. L. Pei and H. B. Han, *Carbon*, 2006, **44**, 496–500.
- 72 C.-Y. Shu, C.-R. Wang, J.-F. Zhang, H. W. Gibson, H. C. Dorn, F. D. Corwin, P. P. Fatouros and T. J. S. Dennis, *Chem. Mater.*, 2008, **20**, 2106–2109.
- 73 R. D. Bolskar, A. F. Benedetto, L. O. Husebo, R. E. Price, E. F. Jackson, S. Wallace, L. J. Wilson and J. M. Alford, *J. Am. Chem. Soc.* 2003, **125**, 5471-5478.
- 74 E. Toth, R. D. Bolskar, A. Borel, G. Gonzalez, L. Helm, A. E. Merbach, B. Sitharaman and L. J. Wilson, *J. Am. Chem. Soc.*, 2005, **127**, 799–805.

-
- 75 C. Y. Shu, E. Y. Zhang, J. F. Xiang, C. F. Zhu, C. R. Wang, X. L. Pei and H. B. Han, *J. Phys. Chem. B*, 2006, **110**, 15597–15601.
- 76 B. Sitharaman, R. D. Bolskar, I. Rusakova and L. J. Wilson, *Nano Lett.*, 2004, **4**, 2373–2378.
- 77 S. Laus, B. Sitharaman, E. Toth, R. D. Bolskar, L. Helm, S. Asokan, M. S., Wong, L. J. Wilson and A. E. Merbach, *J. Am. Chem. Soc.*, 2005, **127**, 9368–9369.
- 78 C. Y. Shu, F. D. Corwin, J. F. Zhang, Z. J. Chen, J. E. Reid, M. H. Sun, W. Xu, J. H. Sim, C. R. Wang, P. P. Fatouros, A. R. Esker, H. W. Gibson and H. C. Dorn, *Bioconjugate Chem.*, 2009, **20**, 1186–1193.
- 79 P. P. Fatouros, F. D. Corwin, Z. J. Chen, W. C. Broaddus, J. L. Tatum, B. Kettenmann, Z. Ge, H. W. Gibson, J. L. Russ, A. P. Leonard, J. C. Duchamp and H. C. Dorn, *Radiology*, 2006, **240**, 756–764.
- 80 J. Zhang, P. P. Fatouros, C. Shu, J. Reid, L. Shantell Owens, T. Cai, H. W. Gibson, G. L. Long, F. D. Corwin, Z.-J. Chen and Harry C. Dorn, *Bioconjugate Chem.*, **2010**, *21*, 610–615.
- 81 D. K. MacFarland, K. L. Walker, R. P. Lenk, S. R. Wilson, K. Kumar, C. L. Kepley and J. R. Garbow, *J. Med. Chem.*, 2008, **51**, 3681–3683.
- 82 E. Y. Zhang, C. Y. Shu, L. Feng and C. R. Wang, *J. Phys. Chem. B*, 2007, **111**, 14223–14226.
- 83 S. Laus, B. Sitharaman, E. Toth, R. D. Bolskar, L. Helm, L. J. Wilson and A. E. Merbach, *J. Phys. Chem. C*, 2007, **111**, 5633–5639.

-
- 84 H. L. Fillmore, M. D. Shultz, S. C. Henderson, P. Cooper, W. C. Broaddus, Z. J. Chen, C. Y. Shu, J. F. Zhang, J. C. Ge, H. C. Dorn, F. Corwin, J. I. Hirsch, J. Wilson and P. P. Fatouros, *Nanomedicine*, 2011, **6**, 449-458.
- 85 K. Braun, L. Dunsch, R. Pipkorn, M. Bock, T. Baeuerle, S.-F. Yang, W. Waldeck, and M. Wiessler, *Int. J. Med. Sci.*, 2010, **7**, 136 -146.
- 86 Y. Horiguchi, S. Kudo and Y. Nagasaki, *Sci. Technol. Adv. Mater.*, 2011, **12**, 044607.

Table 1

Reduction and Oxidation Potentials (in Volts vs Ferrocene/Ferrocinium Ion) for Gadolinium Fullerenes.

Endohedral Fullerene	E_p Red 1	$E_{1/2}$ Red 1	E_p Red 2	$E_{1/2}$ Red 2	E_p Red 3	$E_{1/2}$ Ox 1	$E_{1/2}$ Ox 2	ΔE_{gap}
Gd ₃ N@C ₂ (22010)-C ₇₈ (a)	-1.53		-1.89			+0.47		2.00
GdSc ₂ N@C ₇₈ (b)	-1.44		-1.88			+0.45	0.92	1.89
Gd ₃ N@I _h -C ₈₀ (c)	-1.44		-1.86		-2.15	+0.58		2.02
GdSc ₂ N@I _h -C ₈₀ (b)	-1.32					+0.64		1.96
Gd ₂ ScN@I _h -C ₈₀ (b)	-1.36					+0.66		2.02
Gd ₃ N@I _h -C ₈₂								
Gd ₃ N@C _s (51365)-C ₈₄ (c)	-1.37		-1.76			+0.32		1.69
Gd ₅ ScN@C _s (51365)-C ₈₄ (b)	-1.44		-1.80		-2.08	+0.37	+0.74	1.81
Gd ₃ N@I _h -C ₈₆								
Gd ₃ N@D ₂ (35)-C ₈₈ (c)	-1.43	-1.38	-1.74	-1.69		+0.06	+0.49	1.49
Gd ₂ ScN@D ₂ (35)-C ₈₈ (b)		-1.26		-1.63	-2.05	+0.07	+0.48	1.33

(a) From M. N. Chaur, X. Aparicio-Anglés, B. Q. Mercado, B. Elliott, A. Rodríguez-Forteza, A. Clotet, M. M. Olmstead, A. L. Balch and J. M. Poblet, L. Echegoyen, *J. Phys. Chem. C*, 2010, **114**, 13003–13009.

(b) From A. L. Svitova, A. A. Popov and L. Dunsch, *Inorg. Chem.* 2013, **52**, 3368–3380.

(c) From M. N. Chaur, F. Melin, B. Elliott, A. J. Athans, K. Walker, B. C. Holloway and L. Echegoyen *J. Am. Chem. Soc.*, 2007, **129**, 14826–14829.

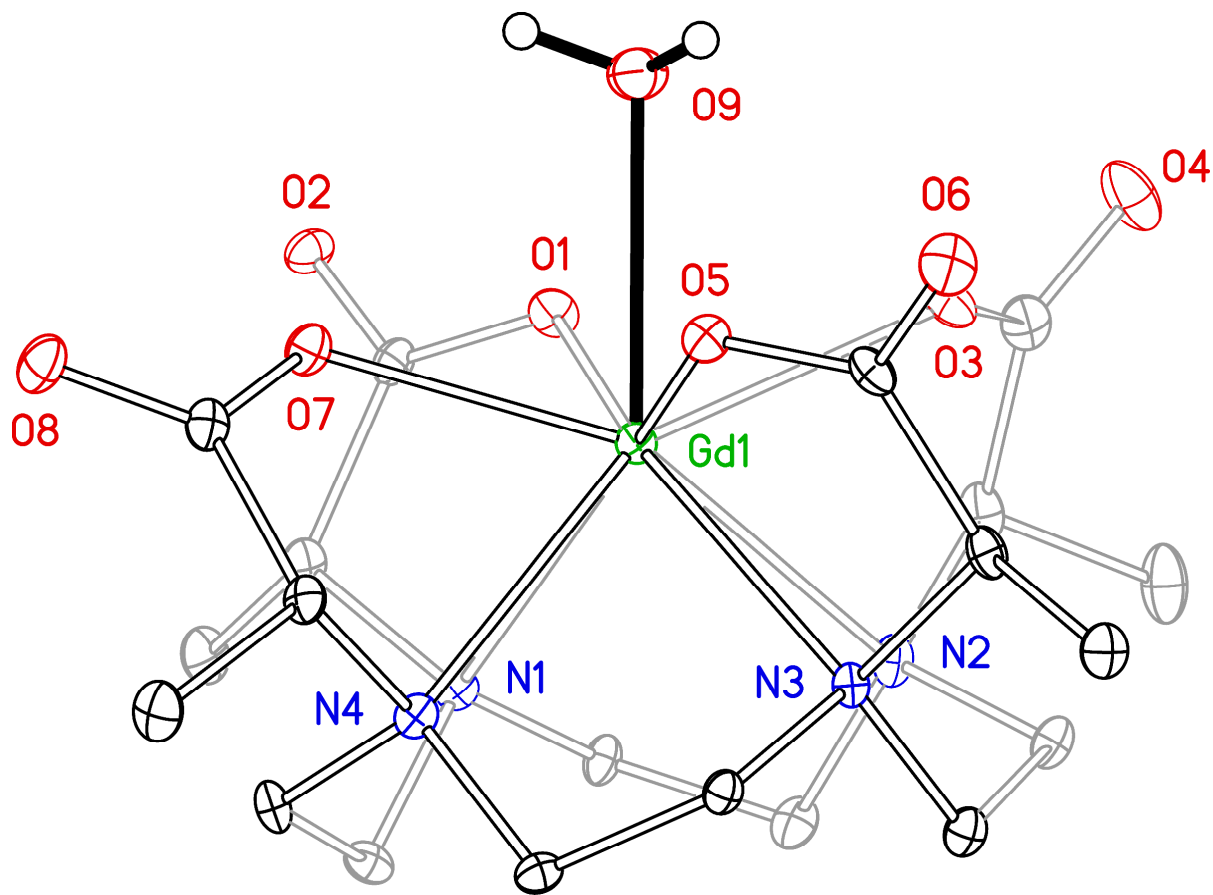


Figure 1. The structure of the anion $[\text{Gd}(\text{DOTMA})(\text{H}_2\text{O})]^-$ in the salt $\text{Na}_4[\text{Gd}(\text{DOTMA})(\text{H}_2\text{O})]_2\text{Cl}_2 \cdot (\text{H}_2\text{O})_{12}$ with oxygen atoms in red and nitrogen atoms in blue. From data in S. Aime, M. Botta, Z. Garda, B. E. Kucera, G. Tircso, V. G. Young and M. Woods, *Inorg. Chem.*, 2011, **50**, 7955–7965

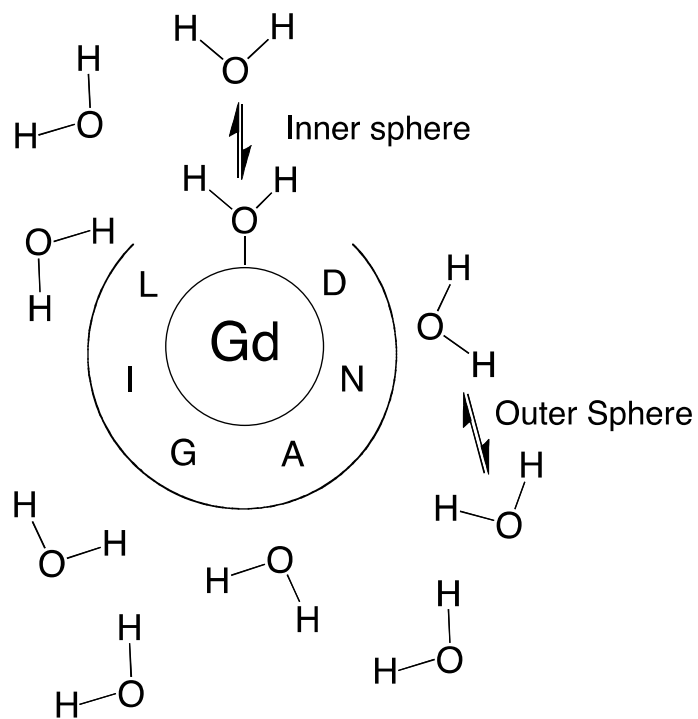


Figure 2. Water exchange processes in chelated gadolinium complexes typically used as MRI relaxation agents.

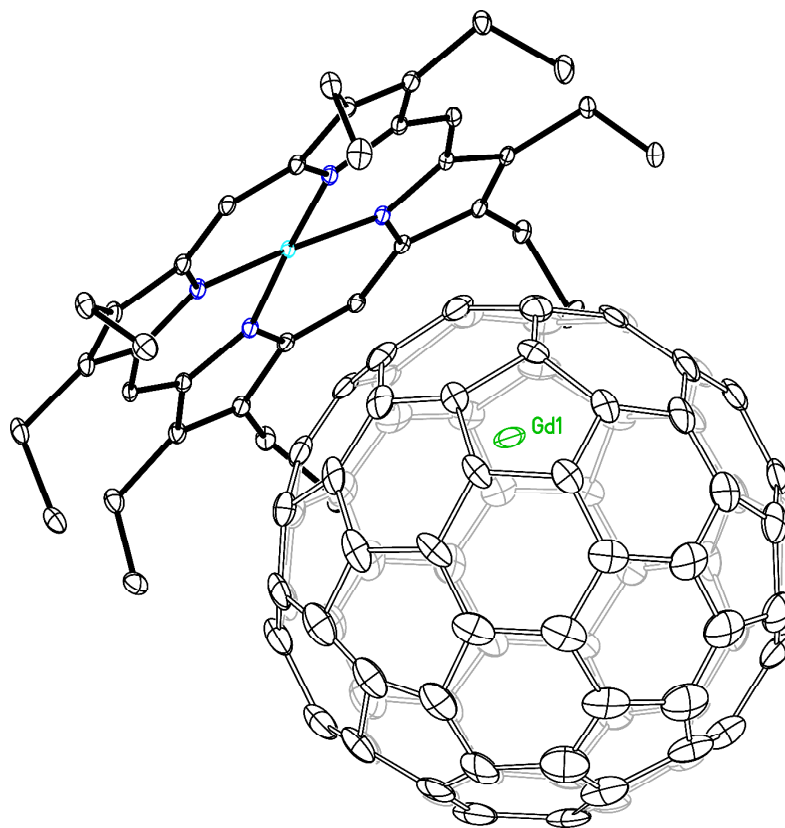


Figure 3. The structure of $\text{Gd}@C_{2v}(9)\text{-C}_{82}$ in a cocrystal with $\text{Ni}(\text{OEP})$. From data in M. Suzuki, X. Lu, S. Sato, H. Nikawa, N. Mizorogi, Z. Slanina, T. Tsuchiya, S. Nagase and T. Akasaka, *Inorg. Chem.* 2012, **51**, 5270–5273.

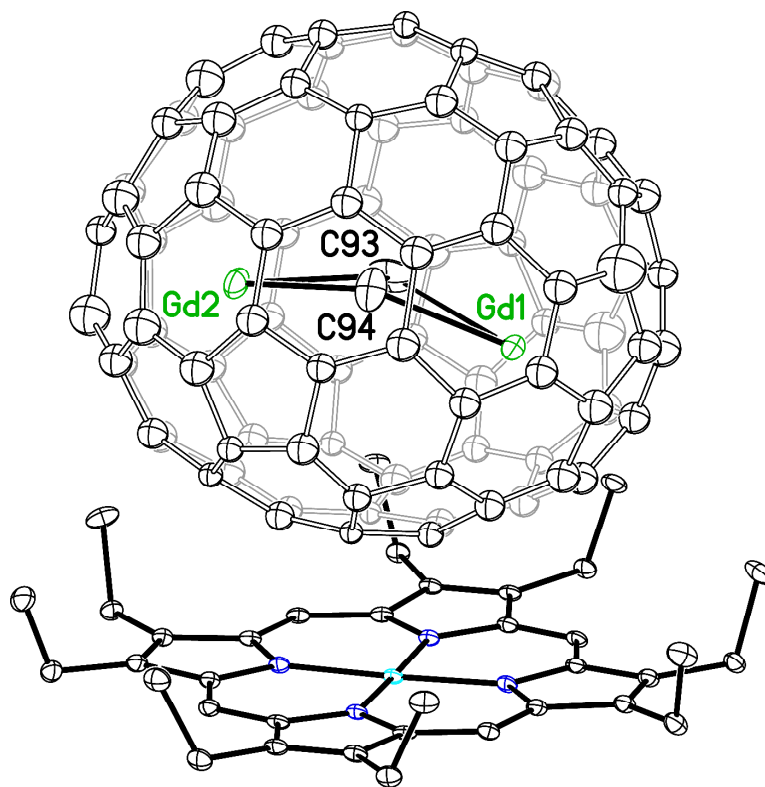


Figure 4. The structure of $\text{Gd}_2\text{C}_2@D_3(85)\text{-C}_{92}$ in $\text{Gd}_2\text{C}_2@D_3(85)\text{-C}_{92} \cdot \text{Ni}(\text{OEP}) \cdot 2\text{C}_6\text{H}_6$. Drawn from the data in H. Yang, C. Lu, Z. Liu, H. Jin, Y. Che, M. M. Olmstead and A. L. Balch, *J. Am. Chem. Soc.*, 2008, **130**, 17296-17300.

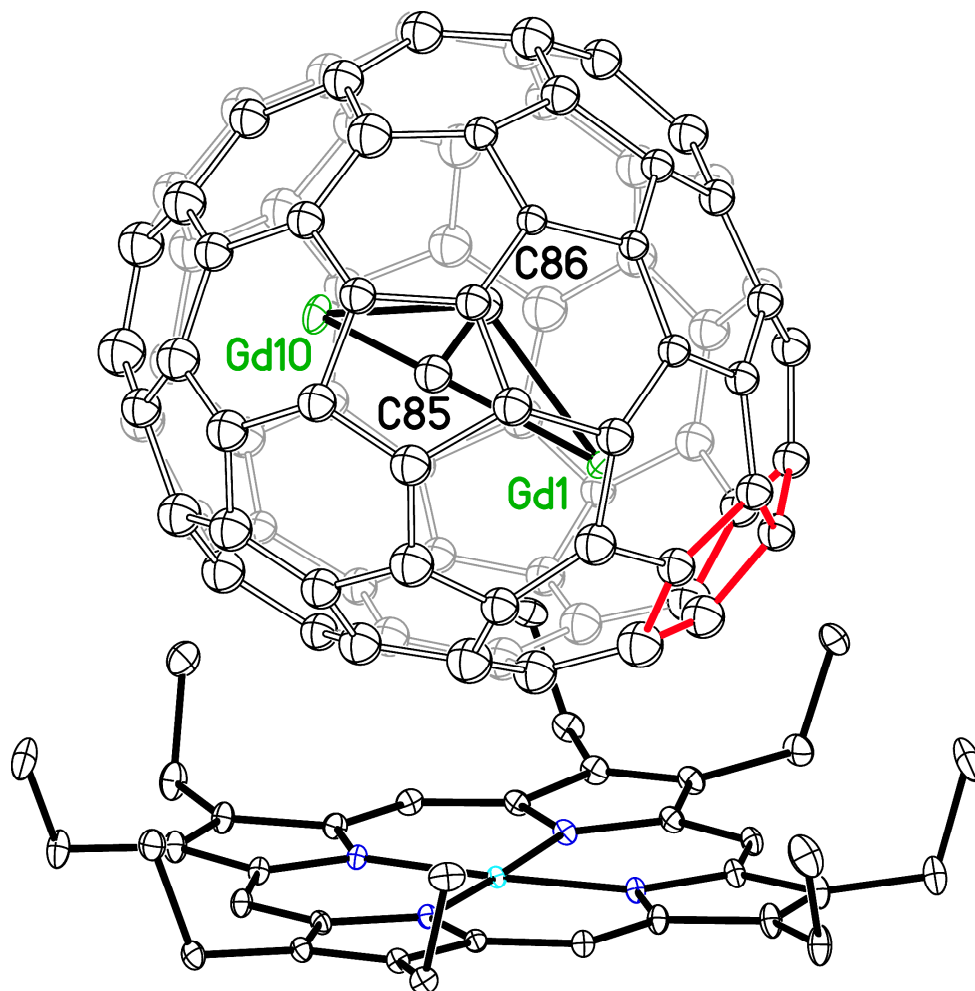


Figure 5. The structure of the non-IPR fullerene $\text{Gd}_2\text{C}_2@C_1(51383)\text{-C}_{84}$ in $\text{Gd}_2\text{C}_2@C_1(51383)\text{-C}_{84}\bullet\text{Ni}(\text{OEP})\bullet 1.75\text{C}_7\text{H}_8\bullet 0.25\text{C}_6\text{H}_6$. The site where two pentagons abut is marked in red. Drawn from the data in J. Zhang, F. L. Bowles, D. W. Bearden, W. K. Ray, T. Fuhrer, Y. Ye, C. Dixon, K. Harich, R. F. Helm, M. M. Olmstead, A. L. Balch and H. C. Dorn, *Nat. Chem.* 2013, **5**, 880-885.

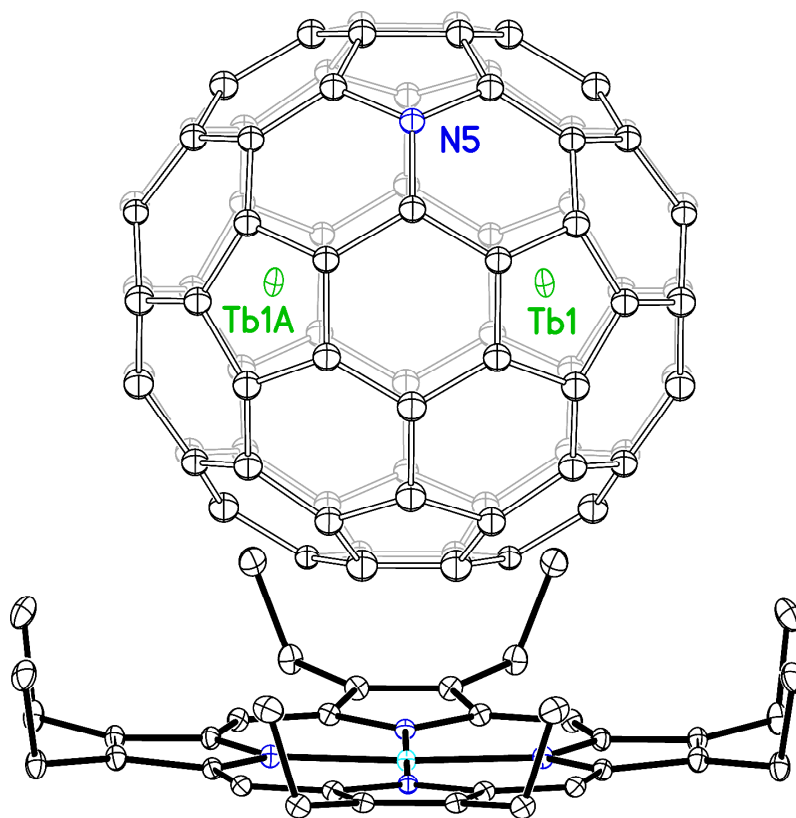


Figure 6. The structure of $\text{Tb}_2@C_{79}\text{N}$, an analog of $\text{Gd}_2@C_{79}\text{N}$. The location of the nitrogen atom in the cage is not known due to the presence of crystallographic disorder. However, computations suggest it is in the position indicated in blue or one of the other sites along the central vertical belt of atoms in the cage. Drawn from the data in T. Zuo, L. Xu, C. M. Beavers, M. M. Olmstead, W. Fu, D. Crawford, A. L. Balch and H. C. Dorn, *J. Am. Chem. Soc.*, 2008, **130**, 12992-12997.

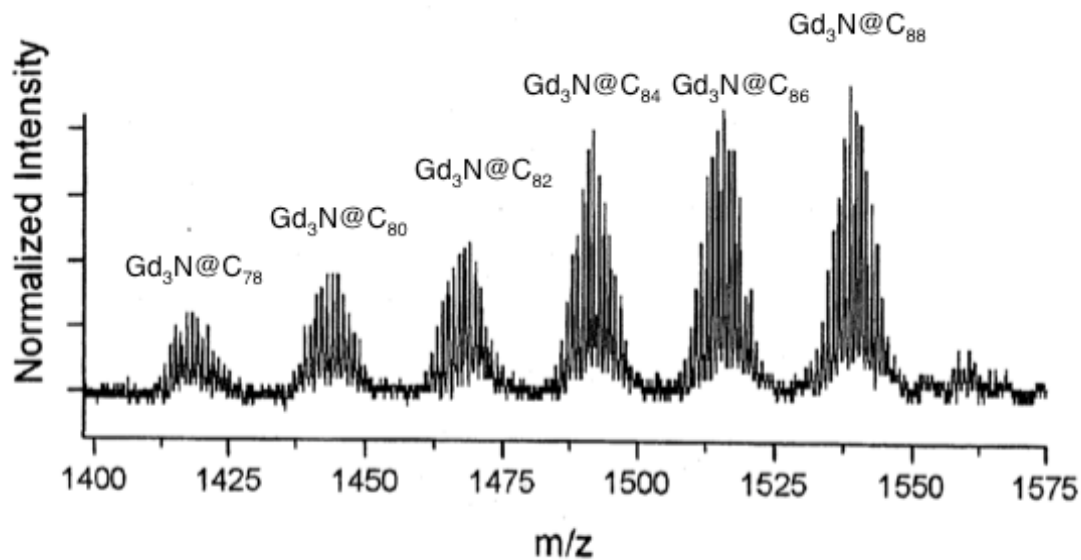


Figure 7. Mass spectrum of the soluble $\text{Gd}_3\text{N}@C_{2n}$ species extracted from raw soot after removal of empty cage fullerenes. From M. N. Chaur, F. Melin, B. Elliott, A. J. Athans, K. Walker, B. C. Holloway and L. Echegoyen *J. Am. Chem. Soc.*, 2007, **129**, 14826-14829.

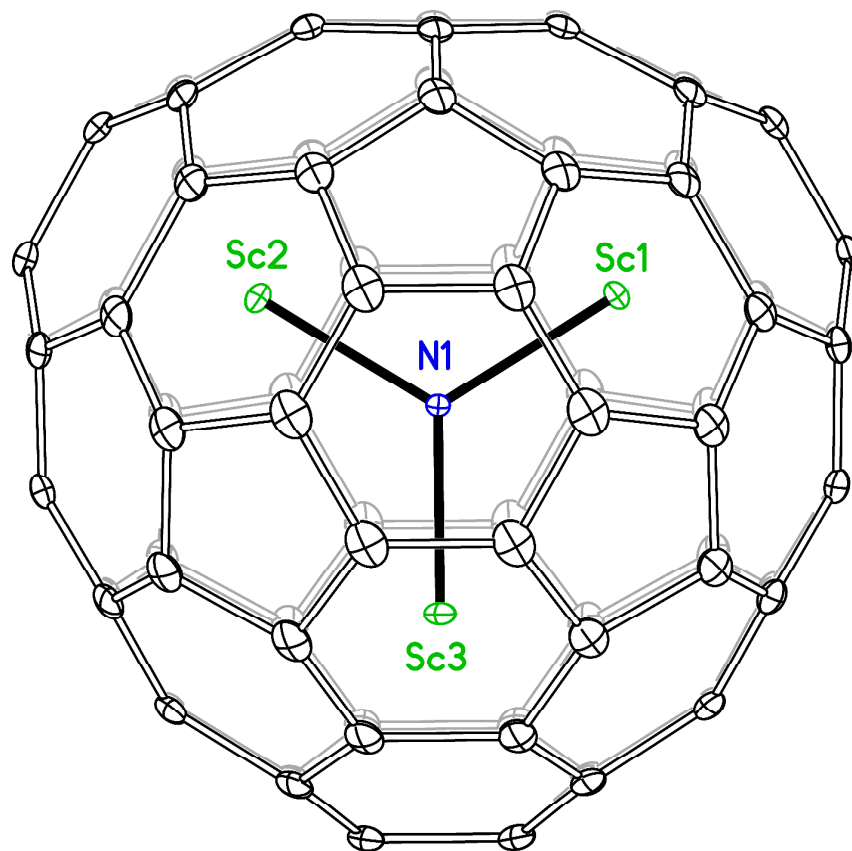


Figure 8. The structure of Sc₃N@D_{3h}(5)-C₇₈ looking down the three-fold axis of the molecule.

Drawn from the data in B. Q. Mercado, M. N. Chaur, L. Echegoyen, J. A. Gharamaleki, M. M. Olmstead and A. L. Balch, *Polyhedron*, 2013, **58**, 129–133.

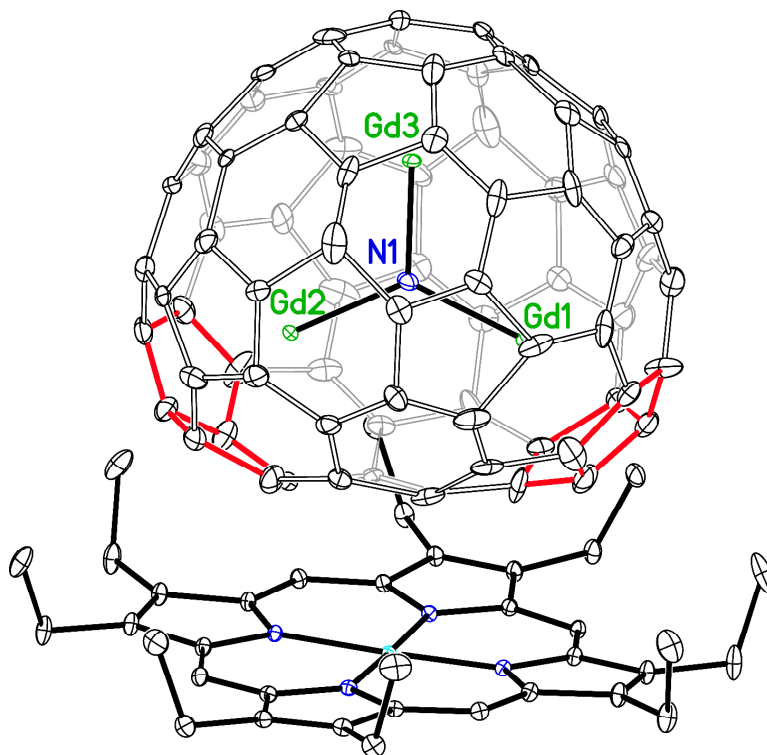


Figure 9. The structure of the non-IPR fullerene $\text{Gd}_3\text{N}@C_2(22010)\text{-C}_{78}$ in $\text{Gd}_3\text{N}@C_2(22010)\text{-C}_{78}\bullet\text{Ni}(\text{OEP})\bullet 1.5\text{C}_6\text{H}_6$. The two sites where two pentagons abut are highlighted in red. Drawn from information in C. M. Beavers, M. N. Chaur, M. M. Olmstead, L. Echegoyen and A. L. Balch, *J. Am. Chem. Soc.*, 2009, **131**, 11519–11524.

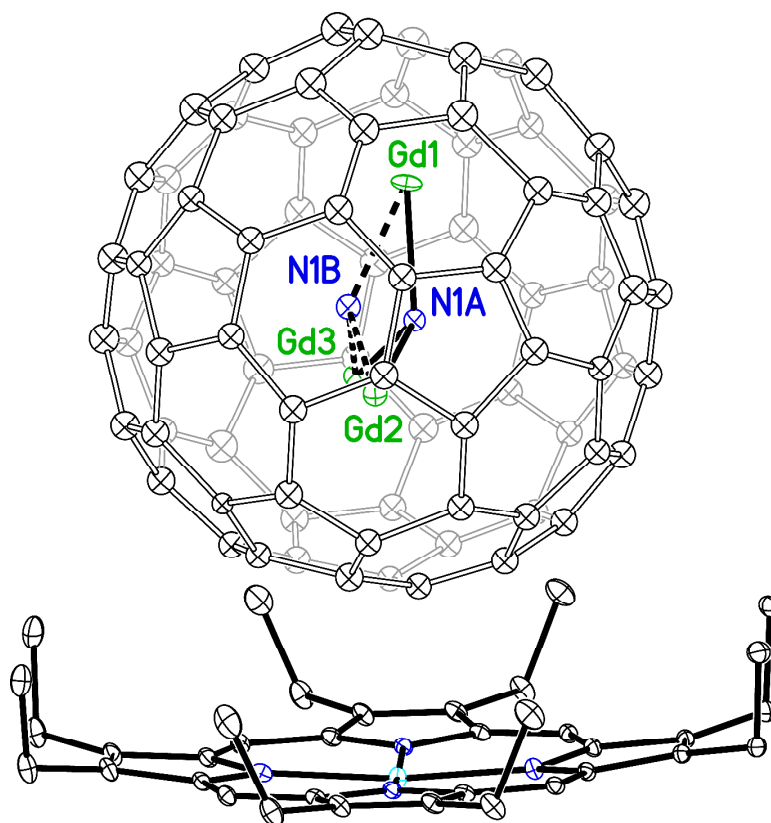


Figure 10. The structure of $\text{Gd}_3\text{N}@I_h\text{-C}_{80}$ showing the major (N1A) and minor (N1B) orientations of the pyramidal unit Gd_3N . Drawn from the data in S. Stevenson, J. P. Phillips, J. E. Reid, M. M. Olmstead, S. P. Rath and A. L. Balch, *Chem. Commun.* 2004, 2814-2815.

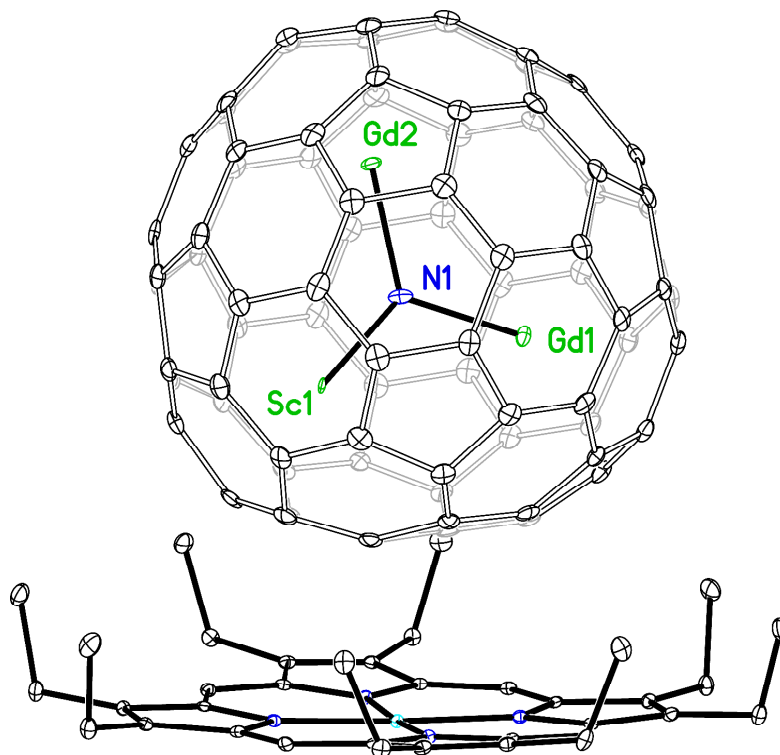


Figure 11. The structure of $\text{Gd}_2\text{ScN}@I_h\text{-C}_{80}$ with the plane of the Gd_2Sc group nearly perpendicular to the porphyrin. Drawn from the data in S. Stevenson, C. J. Chancellor, H. M. Lee, M. M. Olmstead and A. L. Balch, *Inorg. Chem.*, 2008, **47**, 1420-1427.

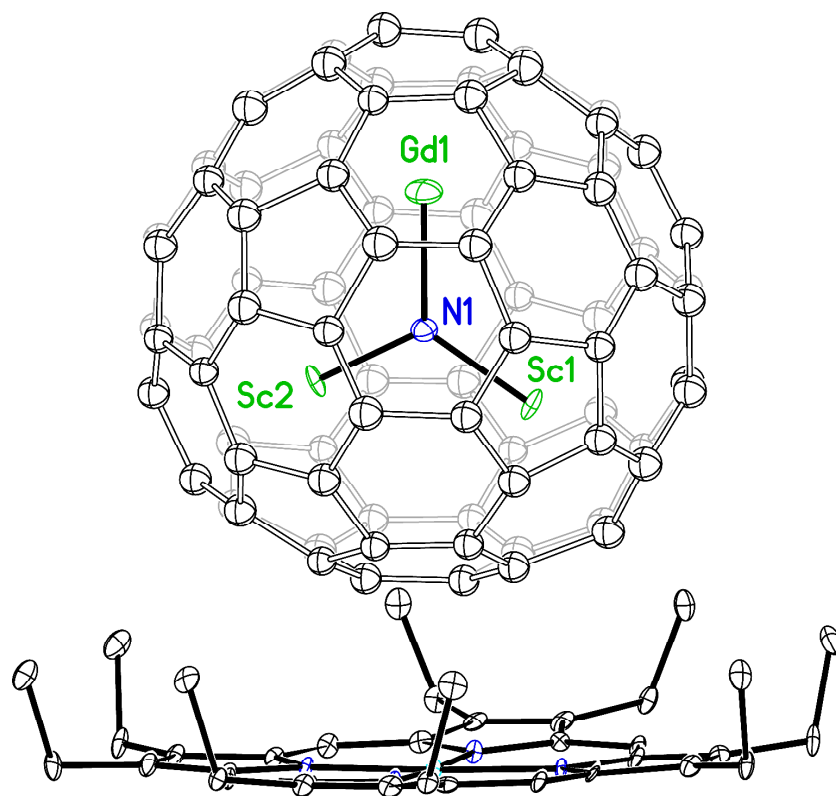


Figure 12. The structure of $\text{GdSc}_2\text{N}@I_h\text{-C}_{80}$ with the plane of the GdSc_2N group nearly perpendicular to the porphyrin. Drawn from the data in S. Stevenson, C. J. Chancellor, H. M. Lee, M. M. Olmstead and A. L. Balch, *Inorg. Chem.*, 2008, **47**, 1420-1427.

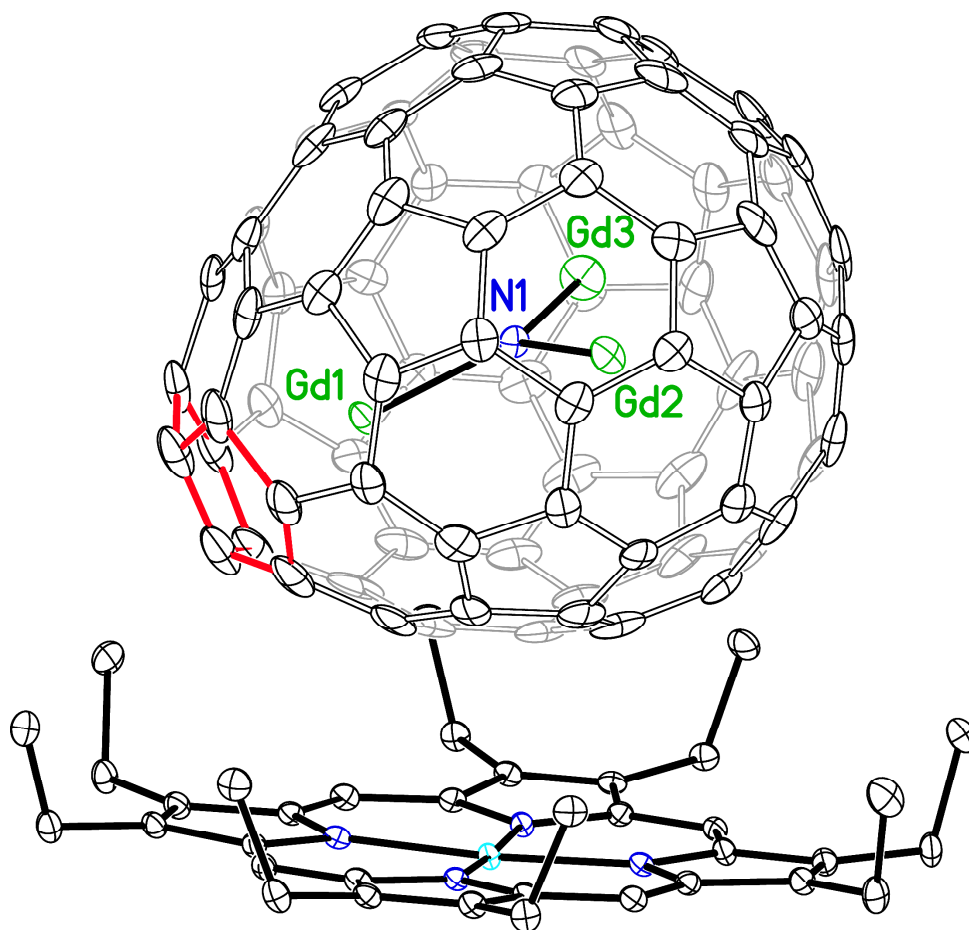


Figure 13. The structure of the non-IPR fullerene $\text{Gd}_3\text{N}@C_5(39663)\text{-C}_{82}$ in $\text{Gd}_3\text{N}@C_5(39663)\text{-C}_{82}\bullet\text{Ni}(\text{OEP})\bullet 2\text{C}_6\text{H}_6$. The single site where two pentagons abut is shown in red. Drawn from the data in B. Q. Mercado, C. M. Beavers, M. M. Olmstead, M. N. Chaur, K. Walker, B. C. Holloway, L. Echegoyen and A.L. Balch, *J. Am. Chem. Soc.*, 2008, **130**, 7854–7855.

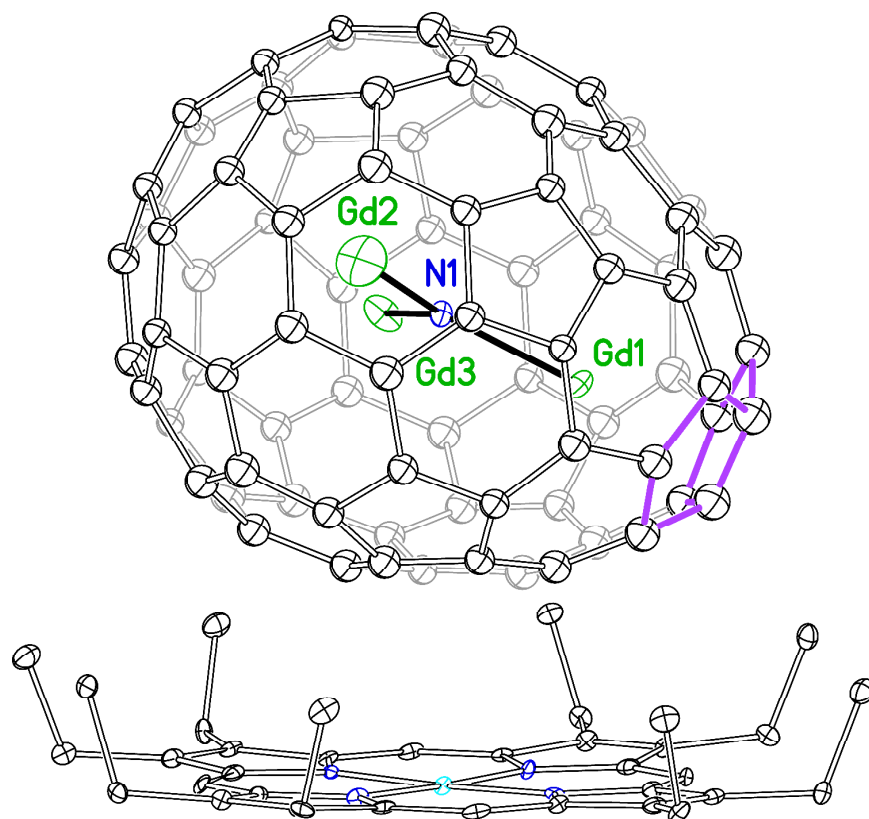


Figure 14. The structure of the non-IPR fullerene $\text{Gd}_3\text{N}@C_5(51365)\text{-C}_{84}$ in $\text{Gd}_3\text{N}@C_5(51365)\text{-C}_{84}\bullet\text{Ni}(\text{OEP})\bullet 2\text{C}_6\text{H}_6$. The site where two pentagons abut is marked in purple. Drawn from the data in T. Zuo, K. Walker, M. M. Olmstead, F. Melin, B. C. Holloway, L. Echegoyen, H. C. Dorn, M. N. Chaur, C. J. Chancellor, C. M. Beavers, A. L. Balch and A. J. Athans, *Chem. Commun.* 2008, 1067-1069.

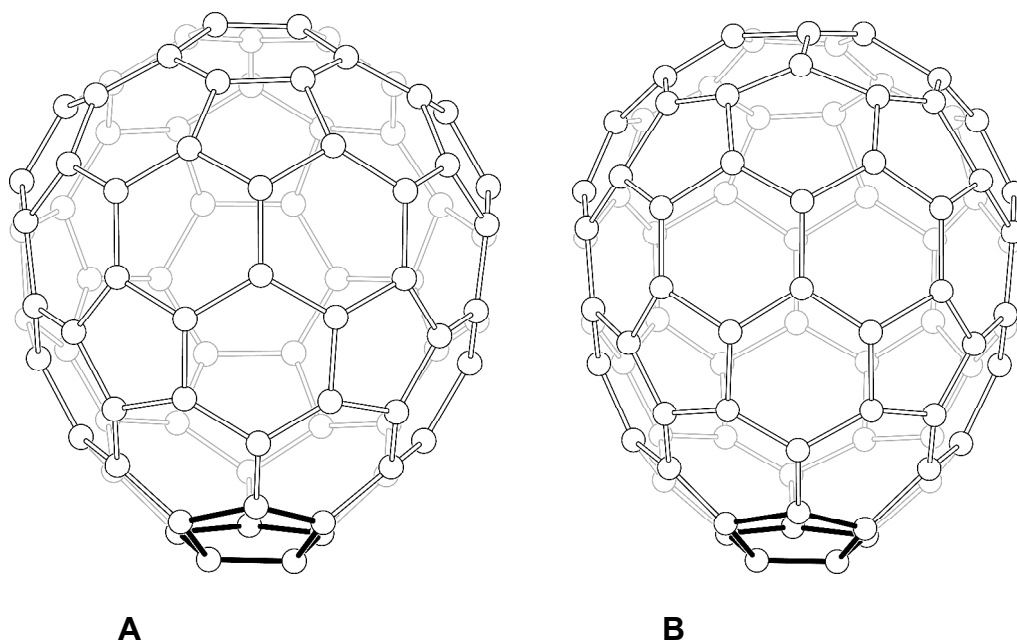


Figure 15. A comparison of the two non-IPR fullerene cages in **A**, $\text{Gd}_3\text{N}@C_s(39663)\text{-C}_{82}$; and **B**, $\text{Gd}_3\text{N}@C_s(51365)\text{-C}_{84}$.

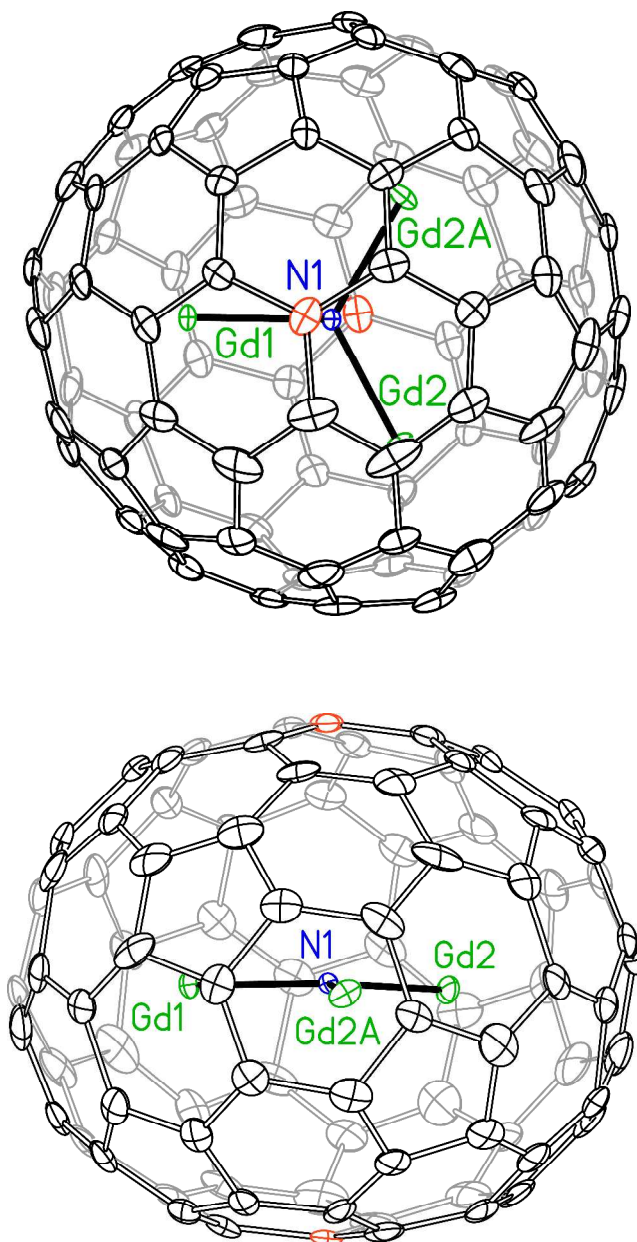


Figure 16. Two orthogonal views of $\text{Gd}_3\text{N}@D_3(17)\text{-C}_{86}$. The upper drawing looks down the three-fold axis, which passes through the two carbon atoms highlighted in orange, while the three fold axis is directed vertically in the lower drawing. Drawn from the data in M. N. Chaur, X. Aparicio-Anglés, B. Q. Mercado, B. Elliott, A. Rodríguez-Forteza, A. Clotet, M. M. Olmstead, A. L. Balch and J. M. Poblet, L. Echegoyen, *J. Phys. Chem. C*, 2010, **114**, 13003–13009.

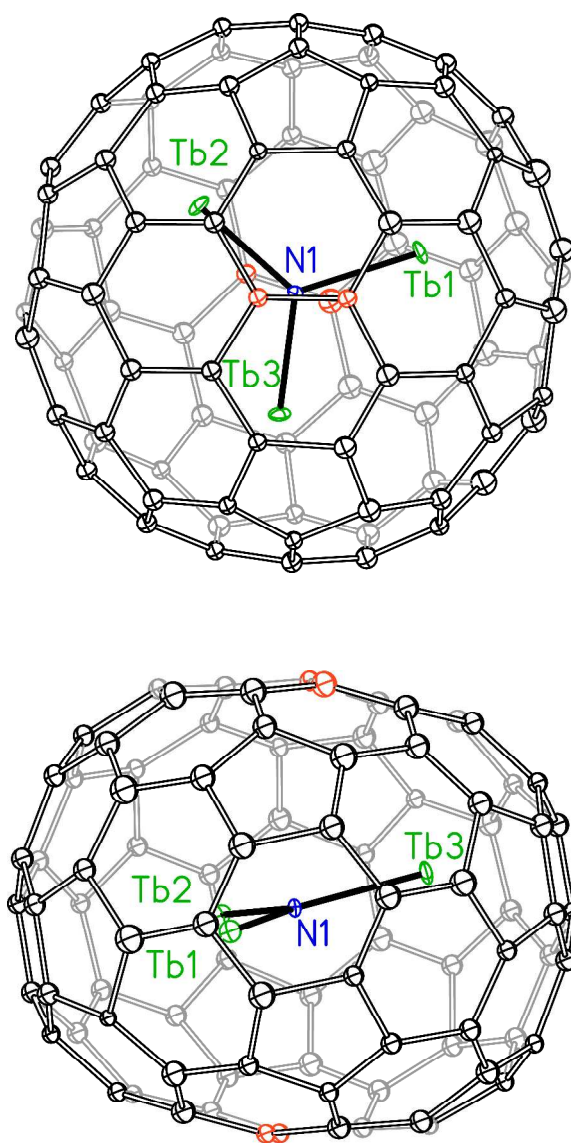


Figure 17. Two orthogonal views of Tb₃N@D₂(35)-C₈₈. Gd₃N@D₂(35)-C₈₈ is expected to have a similar structure. The upper drawing looks down the two-fold axis, which passes between the midpoints between the orange-colored carbon atoms of the cage. In the lower drawing, that two-fold axis is directed nearly vertically. Drawn from the data in T. Zuo, C. M. Beavers, J. C. Duchamp, A. Campbell, H. C. Dorn, M. M. Olmstead and A. L. Balch, *J. Am. Chem. Soc.* 2007, **129**, 2035–2043.

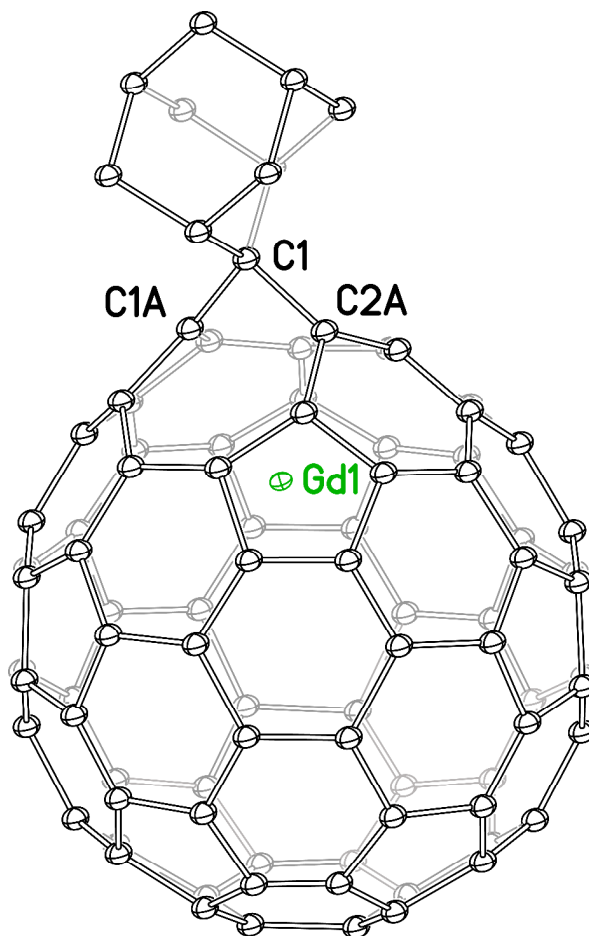


Figure 18. The structure of $\text{Gd}@C_{2v}(9)\text{-C}_{82}(\text{Ad})$. The former two-fold axis of the cage, which has been destroyed by the adduct formation and resulting opening of the C1A-C2A bond, is aligned vertically. Drawn from the data in T. Akasaka, T. Kono, Y. Takematsu, H. Nikawa, T. Nakahodo, T. Wakahara, M. O. Ishitsuka, T. Tsuchiya, Y. Maeda, M. T. H. Liu, K. Yoza, T. Kato, K. Yamamoto, N. Mizorogi, Z. Slanina and S. Nagase, *J. Am. Chem. Soc.* 2008, **130**, 12840–12841.

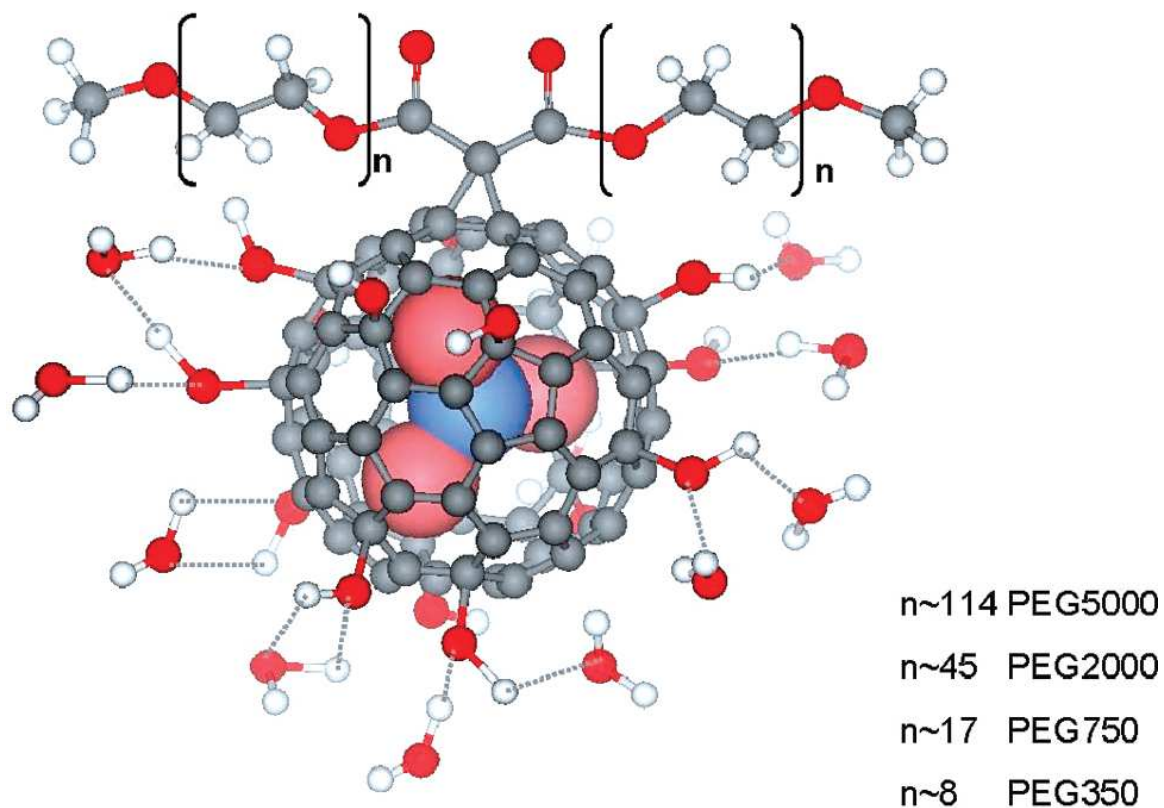


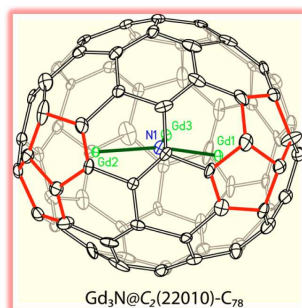
Figure 19. The proposed structure of the $\text{Gd}_3\text{N}@C_{80}[\text{DiPEG}(\text{OH})_x]$ with a few water molecules appended. One Bingel cyclopropanation site is shown at the top while multiple hydroxylation sites and hydrogen bound water molecules cover the rest of the molecule. Reprinted with permission from J. Zhang, P. P. Fatouros, C. Shu, J. Reid, L. Shantell Owens, T. Cai, H. W. Gibson, G. L. Long, F. D. Corwin, Z.-J. Chen and Harry C. Dorn, *Bioconjugate Chem.*, **2010**, *21*, 610–615. Copyright 2010 American Chemical Society.

A table of contents entry

Text

The structures and properties of gadolinium-containing endohedral fullerenes as magnetic resonance imaging (MRI) contrast agents are reviewed here.

Color Graphic



A table of contents entry

Text

The structures and properties of gadolinium-containing endohedral fullerenes as magnetic resonance imaging (MRI) contrast agents are reviewed here.

Color Graphic

